The Determination of Q_{L_g} and Q_C as a Function of Frequency in the Crust of Virginia and its Environs

by

Melissa J. B. Rogers

Thesis submitted to the Faculty of the
Virginia Polytechnic Institute and State University
in partial fulfillment of the requirements for the degree of
Masters of Science
in
Department of Geological Sciences

APPROVED:

G. A. Bollinger, Chairman

J. Arthur Snoke

Cahit Çoruh

Martin C. Chapman

May 13, 1988

Blacksburg, Virginia

The Determination of Q_{L_g} and Q_C

as a Function of Frequency

in the Crust of

Virginia and its Environs

by

Melissa J. B. Rogers

G. A. Bollinger, Chairman

Department of Geological Sciences

(ABSTRACT)

Estimates of the apparent quality factors Q_{L_g} (attenuation determined from the spatial decay of Lg waves) and Q_C (attenuation determined from the temporal decay of seismic coda waves) are made for the crust of Virginia and its environs. The results are presented in the form $Q_{(L_g,C)}(f) = Q_o f^N$, where $Q_o = Q_{(L_g,C)}(1\ Hz)$ and N represents the frequency dependence. The study area is located in the Appalachian region of Virginia and eastern Tennessee, containing three areas of regionally high seismicity: the central Virginia, Giles County, and eastern Tennessee seismic zones.

The attenuation of the Lg phase was studied using vertical component digital recordings from Virginia Tech Seismological Observatory network stations. The seismic sources were ten regional surface mine explosions and six regional earthquakes. It was determined that Q_{L_g} can be represented by $Q_o = 186$, $\sigma_{\log Q_o} = 0.05$, and $N = 1.1 \pm 0.1$ for the frequency band 1 - 4 Hz.

A site effect corrected estimate of Q_{L_g} was also determined for the study area. This was accomplished using a spectral ratio method in which station site effects and instrument responses are canceled out. For the frequency band 1 - 10 Hz the site independent apparent quality factor can be represented by $Q_o = 155$, $\sigma_{\log Q_o} = 0.1$, and $N = 1.2 \pm 0.2$. Station site factors were estimated using a mean residual technique.

The decay of seismic coda waves across the Giles County, Virginia seismic network was studied to estimate Q_C for western Virginia. A relatively new spectral method was used. The seismic sources were four local earthquakes. For the frequency band 1 - 10 Hz, the results can be re-

presented by $Q_o = 111$, $\sigma_{\log Q_o} = 0.07$, and $N = 1.3 \pm 0.07$. These values agree with a limited number of results obtained using a bandpass, time domain method which showed $Q_o = 132$, $N = 1.3$.

The results obtained for the Virginia area differ significantly in the 1 - 3 Hz range from those reported in most previous studies of the eastern United States. Previous studies have generally shown $800 \leq Q_o \leq 1000$ and $0.3 \leq N \leq 0.5$, but many of those results are for much larger regions and determined using different analysis techniques.

Several reasons that could account for the different results include **1)** estimates of attenuation may be affected by incorrect geometrical spreading models, **2)** the size of the study area may affect the estimates, and **3)** estimates of $Q_{(L_g,C)}$ made for broad regions may be biased by zones of differing tectonic activity. Of these factors, only the effects of changing geometrical spreading coefficients and scattering models (related to study area) can be quantified. Neither of these affect the results by more than a factor of two.

The high frequency dependence values ($N \simeq 1.1$) are probably influenced by the lack of definition of higher frequency ($\simeq 10$ Hz) data at the path distances studied. Future studies should employ more extensive data sets covering a larger geographic area. At greater distances, the attenuation of higher frequency waves may be more easily observable.

The large frequency dependence values are probably indicative of an area where scattering dominates over anelastic attenuation. The folded and thrusted Appalachian provinces may, indeed, be such a region of high scattering. Such a mechanism may also help to explain southeastern United States meizoseismal areas that are small relative to the total felt areas.

Large frequency dependence results for Q_{L_g} and Q_C are relevant with respect to seismic hazard. We do not believe the results are overly biased by station site effects or varying source effects and if they hold for magnitudes greater than those studied here ($m < 4.2$) , they indicate a greater potential for damage by higher frequency waves to engineering structures in Virginia and its environs than previously assumed.

Acknowledgements

There are numerous people who have helped to make this project a reality. To begin with, I would like to thank Dr. G. A. Bollinger for suggesting the project and giving helpful suggestions and financial support along the way. Martin Chapman performed preliminary Q_{L_g} and Q_C research in the area and wrote several of the key computer programs used in the study. His support throughout this project has been tremendous. I would also like to thank my other committee members, Drs. J. A. Snoke and C. Çoruh for all their valuable assistance in the completion of this work.

This work could not have been completed without the input of the staff of the Virginia Tech Seismological Observatory: Matt Sibol, Ellen Mathena, and Bob Carner.

The conversations and competition in the geophysics graduate student office have contributed to an exceptional learning and growing experience. I would particularly like to thank Rick, Ron, and Sandee for all the times spent working and not working together.

Without the support (both moral and financial) of my parents, Melville and Mary Bodé, I would never have made it through. A special thanks to my husband, Steve, for having the patience to let me finish.

This research was supported in part by the Nuclear Regulatory Commission under contracts NRC-04-134 and NRC-04-85-121.

This thesis is dedicated to my sister, Carolynn Medalie,

who always knows what to say.

And when to say nothing at all.

Thanks for being there, Lynn.

Table of Contents

Introduction 1

Loss mechanisms and the quality factor Q 1

Introduction to problem 4

Site effects 5

Previous work 14

Regional geology 15

The Spectral Analysis of Q_{Lg} and Q_C **21**

Lg spectral method 21

Coda wave method 22

Site Effects **25**

Site response measurements 25

Site effect analysis 26

Data Analysis **31**

Q_{Lg} 31

Q_C 41

Results **46**

Q_{Lg} 46

Q_C 49

Discussion **53**

Q_{Lg} 53

Q_C 55

Q_{Lg} compared with Q_C 55

Comparison of regional results 57

Conclusions 68

Summary **72**

References **75**

Appendix A. Derivation of spectral models **80**

Intrinsic absorption model 80

Geometrical spreading model 82

Scattering model 83

Appendix B. Basic data **85**

Appendix C. Windowing Techniques **87**

Appendix D. Relative Station Site Responses **91**

References 93

Vita 95

List of Illustrations

Figure 1. The Virginia Tech Seismological Observatory network 6
Figure 2. The Lg Q study area 8
Figure 3. Sources and stations used in the RTSM study 10
Figure 4. Coda Q study area 12
Figure 5. Area studied in Lg and coda Q analyses 13
Figure 6. Physiographic provinces of the Appalachian mountains 18
Figure 7. Station - source configuration for the Reversed Two Station Method 29
Figure 8. Typical explosion seismogram from Lg Q analysis 32
Figure 9. Signal and noise spectra for a typical Lg event 34
Figure 10. Lg spectra of an event from Central Virginia stations 35
Figure 11. Lg spectra of an event at various distances 36
Figure 12. (log A + 0.5 log R) vs t 38
Figure 13. Station site responses for VTSO station HWV 40
Figure 14. Typical seismograms from coda Q analysis 43
Figure 15. Signal and noise spectra for a typical coda event 44
Figure 16. (log t^2 P) vs t 45
Figure 17. Q_{Lg} results from the Lg spectral method 47
Figure 18. Q_{Lg} results from RTSM 48
Figure 19. Q_C results for four earthquakes 51
Figure 20. Q_C results from the two analysis methods 52
Figure 21. Q_{Lg} and Q_C results from the different analyses 56

Figure 22. Q_{Lg} and Q_c for the eastern United States 60
Figure 23. The effect of changing geometrical spreading correction on Q_{Lg} results 62
Figure 24. Study area from Gupta and McLaughlin (1987) 66
Figure 25. Amplitude spectra generated using the different windows tested 89
Figure 26. Q_{Lg} values generated using the different windows tested 90

List of Tables

Table 1. Epicentral data for events used in Lg spectral method. 7

Table 2. Epicentral data for events used in the RTSM analysis. 9

Table 3. Epicentral data for events used in coda Q analysis. 11

Table 4. Worldwide variations of Lg Q and coda Q. 16

Table 5. Eastern United States variations of Lg Q and coda Q. 17

Table 6. Lg and coda Q results for the eastern United States. 58

Table 7. Values of Q_c for the United States standardized to 6 Hz. 59

Table 8. Seismogram computer files used in this study. 86

Introduction

Loss mechanisms and the quality factor Q

As a seismic wave propagates from its source region, energy is redistributed throughout the medium by geometrical spreading and scattering and lost through conversion to heat. Geometrical spreading causes a decrease in wave amplitude along a path as the initial wave energy is spread out over an increasingly larger wavefront. Amplitude may also be affected by scattering, reflection, and conversion of wave types as the wave encounters heterogeneities in the earth, but there is no loss of total energy. Several in depth summaries of seismic wave attenuation mechanisms have been published (Jackson and Anderson, 1970; Stacey and others, 1975; Liu and others, 1976; Kanamori and Anderson, 1977; Johnston and others, 1979). These references contain discussions of scattering and four actual loss (internal friction) mechanisms: damped resonance, static hysteresis, relaxation, and viscosity. Of the four loss categories listed, the above papers consider static hysteresis and relaxation mechanisms to be likely causes of energy attenuation in the frequency range 1 - 10 Hz, the range of interest in this study. Damped resonance of dislocations explains internal friction at megacycle frequencies only. The processes involved in viscosity losses are poorly understood and may or may not be of consequence in this frequency range.

Static hysteresis internal friction results when stresses cause a change in the condition of a solid that is not completely reversed upon removal of the stresses. The internal friction caused by such processes is amplitude dependent and, in many cases, frequency independent. An example of such a mechanism is sliding friction - the dissipation of energy by friction across partially closed cracks.

Relaxation internal friction occurs when applied stress causes a change in the physical condition of a solid that is reversed upon removal of stress. The processes act to relieve instantaneous stress and this causes internal friction that is linear and frequency dependent. Examples of such processes are thermoelastic heating, fluid flow in pores, and phase changes.

The actual loss of energy (intrinsic attenuation) with propagation may be described by the quality factor Q. The quality factor is defined as the the inverse of the dimensionless dissipation coefficient for a volume of material subjected to cyclic stress at a frequency ω:

$$\frac{1}{Q} = -\frac{\Delta E}{2\pi E}, \qquad [1]$$

where ΔE is the change in strain energy per cycle (energy is lost because of imperfections in the elasticity of the material, hence ΔE is negative) and E is the peak strain energy stored in the volume. Q is bounded by zero and infinity, as dictated by the negative sign in equation (1). As $Q \rightarrow \infty$, the material approaches perfect elasticity; waves are not attenuated as they propagate.

Values of Q have been measured for a number of media using various techniques. Methods of Q determination include the study of the decay of free and driven oscillations where it is necessary to know or assume the nature of a substance's elastic moduli, resonance frequency, and other internal properties. Laboratory measurements of the quality factor for various rock types have been performed (Knopoff, 1964; Sato and Manghanani, 1985; Toksöz and others, 1979). Waters (1981, p. 29) gives a compilation of Q values for various rock types. Laboratory measurements have at times been contradictory, some showing that for dry rock samples Q is essentially independent of frequency over portions of the broad frequency range 1 Hz - 1.5 MHz (e.g., Knopoff, 1964), while others show that Q is frequency dependent at least in the MHz range (e.g., Sato and Manghanani, 1985).

Extension of such laboratory measurements to the crust of the earth may not be directly possible. Several differences between the laboratory and the earth must be considered. The sizes of laboratory samples and the wavelengths and frequencies studied are not necessarily representative of seismic wave propagation through the earth's crust. The temperature and pressure conditions and rock fluid content in the laboratory also may not be representative of the *in situ* properties of the earth.

Studies of the quality factor in the earth using spherical and torsional earth modes and P waves of large ($m \simeq 7$) earthquakes have resulted in values of Q for the mantle that are frequency independent (Nowroozi, 1968; Teng, 1968). Constant values of Q are often assumed in many earthquake studies focusing on source parameters and earth structure (e.g., Sacks and Snoke, 1984; Dysart and others, 1988).

Several attenuation studies in the last ten years, however, have determined empirically that 'the quality factor' is frequency dependent in the range 1 - 10 Hz (e.g., Pulli, 1984; Hasegawa, 1985; Chávez and Priestley, 1986). These studies have looked at the decay of body and surface waves of local and regional earthquakes and explosions. The frequency dependent quality factors observed in these studies are believed to be not solely measures of intrinsic absorption, but rather estimates of more complex attenuation mechanisms.

Dainty and Toksöz (1981) consider the observed quality factor of coda waves (backscattered body waves to be discussed later in this section) to have two components: $\frac{1}{Q} = \frac{1}{Q_i} + \frac{1}{Q_s}$ where $\frac{1}{Q_i}$ is the contribution from intrinsic absorption and $\frac{1}{Q_s}$ is the contribution from scattering. Q_i is considered frequency independent; the observed frequency dependence of Q for coda waves is due solely to the scattering component (Aki, 1980). The presence of scattering effects in observed quality factors necessitates the introduction of such terms as Q_{Lg} and Q_C, used here to represent the observed quality factors based on Lg phase decay studies and coda wave decay studies, respectively. Note that observed values such as Q_{Lg} and Q_C are not solely a measure of intrinsic absorption, but probably contain both scattering and absorption effects, the separation of which is difficult to achieve.

Introduction to problem

Several recent attenuation studies have resulted in observed quality factors that are frequency dependent in the range 1 - 10 Hz (e.g., Pulli, 1984; Hasegawa, 1985; Chávez and Priestley, 1986). These studies have mostly involved the attenuation of the Lg phase, resulting in Q_{L_g} values, and the attenuation of coda waves, resulting in Q_C values. As originally defined (Press and Ewing, 1952), the Lg phase is a surface wave having a group velocity of $\simeq 3.51 \pm 0.07$ km/sec, initial periods of 0.5 to 6.0 seconds, and sharp onsets. The wave arrival is usually identified by the largest amplitude portion of a seismic trace for events that have mainly continental travel paths. Campillo and others (1985) consider the Lg phase to be a surface wave composed of multiple supercritically reflected S waves which sample the crust or a crustal low velocity channel. In this study, the term *Lg phase* is applied to the largest amplitude portion of a seismic event at local and regional distances on the short period, vertical component seismogram. The theory of Aki (1969) and Aki and Chouet (1975), models the coda of local seismic signals as primary waves scattered by heterogeneities in the earth. The coda of a local earthquake is considered to be the result of S-to-S singly backscattered waves in an infinite, homogeneous, isotropic medium in which heterogeneities are randomly and uniformly distributed, see Appendix A. Both Q_{L_g} and Q_C have been observed to vary with frequency as $Q_{(L_g,C)}(f) = Q_o f^N$ where Q_o is $Q_{(L_g,C)}(1\ Hz)$, f is seismic frequency, and N is the power law frequency dependence.

This study was designed to determine Q_{L_g} and Q_C in the frequency range 1 - 10 Hz for the crust of Virginia and its environs. Because damage to structures is caused primarily by strong motion in this frequency band (Nuttli, 1978), knowledge of attenuation at these frequencies is important for seismic hazard assessment.

The attenuation of the Lg phase (group velocity = 3.5 km/sec) was studied using vertical component digital recordings from Virginia Tech Seismological Observatory (VTSO) network stations, Figure 1. Bollinger and others (1986) give a detailed description of the VTSO network. The sources used in the Q_{L_g} analysis were ten regional surface mine explosions in the distance range

250 to 450 km and six regional earthquakes in the distance range 150 to 650 km with focal depths 3.5 to 26 km and magnitudes 3.3 to 4.2 (Figure 2, Table 1). The values of Q_{Lg} were determined from the decay of the Lg phase across the seismic network. Data from the sixteen events studied were combined to estimate regional values of Q_{Lg} at frequencies from 1 to 10 Hz. Separate estimates of Q_{Lg} were also made from blast data and earthquake data.

Estimates of Q_{Lg} that are free from site effect contamination were also obtained for the Virginia area. The method used involves the calculation of spectral ratios from several source - station groupings (Chun and others, 1987). Three regional sources and seven VTSO stations were used in the analysis (Figure 3, Table 2). Epicentral distances ranged from about 35 to 500 km.

The decay of coda waves from four local earthquakes in the magnitude range 2.1 to 3.2, focal depth range 3 to 15 km, and epicentral distance range 6 to 260 km was studied to estimate Q_C in the crust of western Virginia (Figure 4, Table 3). Estimates of Q_C were derived for all stations recording an event from the temporal decay of the power spectra according to the single scattering model of Aki and Chouet (1975). A relatively new spectral method of analysis was used. The data from the four earthquakes were combined to estimate Q_C for the crust of western Virginia. Additional estimates of Q_C were obtained using one of the local earthquakes as recorded at four stations. A classic time domain method of analysis was used as a check on the validity of the power spectral method.

Figure 5 shows a map view of source - station ray paths for the entire attenuation study. This provides an idea of the extent of the study area - western and central Virginia, eastern Tennessee, western North Carolina, eastern Kentucky, and southern West Virginia.

Site effects

Attenuation studies are usually performed using data collected at several different seismic recording stations. Numerous studies have shown that the seismograms of an earthquake recorded at stations on different geologic formations and in areas of different topography vary significantly

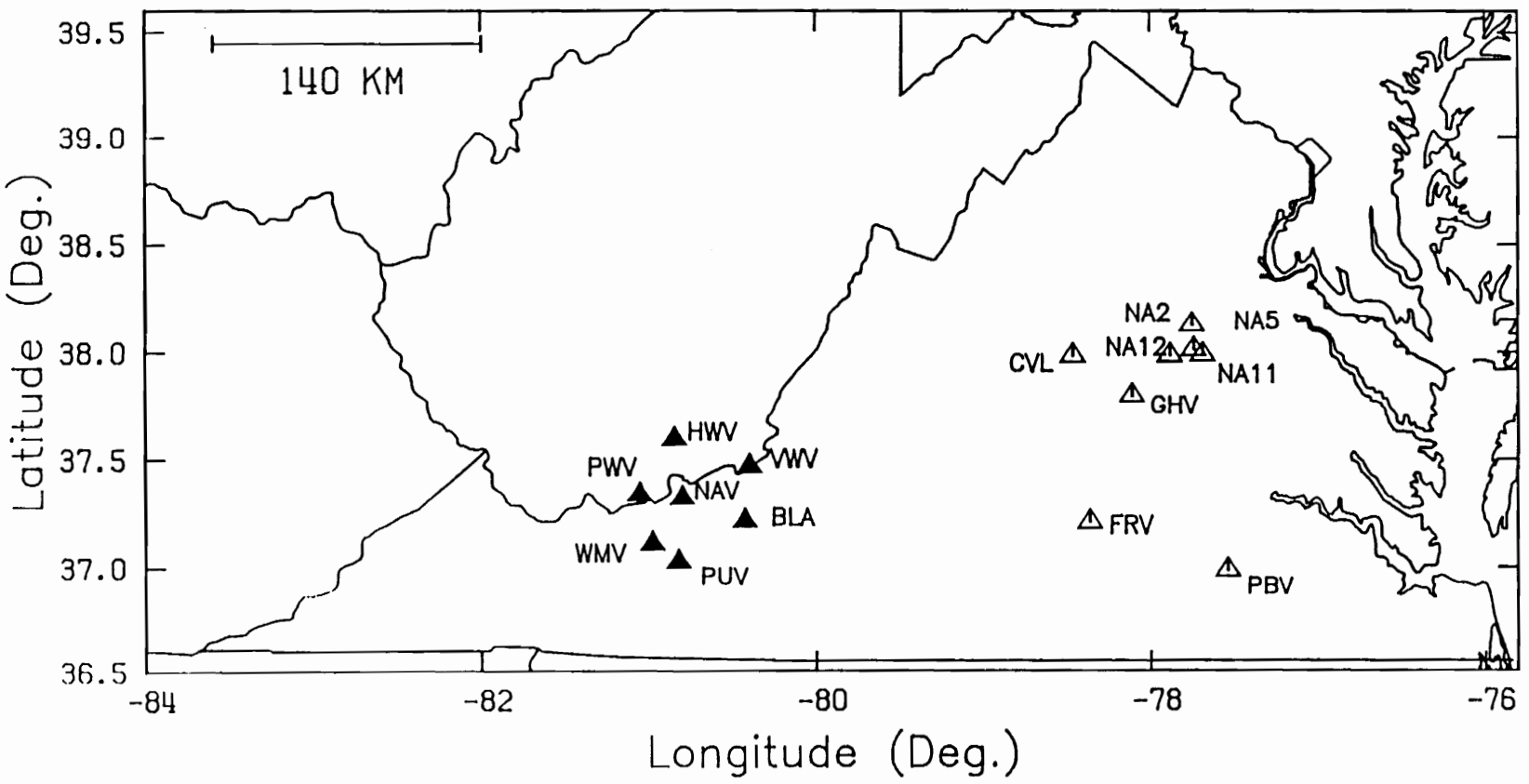

Figure 1. The Virginia Tech Seismological Observatory network: Virginia Tech Seismological Observatory (VTSO) stations. Giles County, Virginia subnetwork stations are shown as solid triangles; central Virginia subnetwork stations are shown as open triangles.

Table 1. Epicentral data for events used in Lg spectral method.

REGIONAL BLASTS

Event Number	Date (M-D-Y)	Location (Deg)	Origin Time (UTC)	Distance (km)
861092033	04-19-86	37.41N 83.37W	20h-33m-12.27s	206-506
861171242	04-27-86	37.35N 83.28W	12h-43m-14.47s	198-496
861502047	05-30-86	37.28N 83.18W	20h-46m-37.02s	189-485
861642054	06-13-86	37.35N 83.51W	20h-53m-36.39s	217-512
861642119	06-13-86	37.40N 83.30W	21h-18m-30.30s	200-501
861662134	06-15-86	37.30N 83.30W	21h-33m-35.30s	201-496
861821502	07-01-86	37.49N 83.23W	15h-01m-50.37s	194-485
862101946	07-29-86	37.60N 83.20W	19h-44m-57.72s	191-481
862132312	08-01-86	37.50N 83.20W	23h-12m-49.79s	195-483
862322325	08-20-86	37.40N 82.70W	23h-25m-21.72s	144-405

REGIONAL EARTHQUAKES

Event	Date (M-D-Y)	Location (Deg)	Depth (km)	Magnitude (M_D)	Origin Time (UTC)	Distance (km)
870860730	03-27-87	35.58N 84.27W	5	4.2	07h-29m-28.7s	340-640
871920005	07-11-87	36.10N 83.82W	26	3.3	00h-04m-29.4s	277-583
873311859	11-27-87	36.85N 83.10W	15	3.5	18h-58m-29.5s	190-494
880090109	01-09-88	35.27N 84.20W	12	3.3	01h-07m-40.7s	360-638
880471527	02-16-88	36.60N 82.29W	3.5	3.3	15h-26m-54.8s	130-435
880490038	02-18-88	35.33N 83.84W	5	3.3	00h-37m-45.44s	323-624

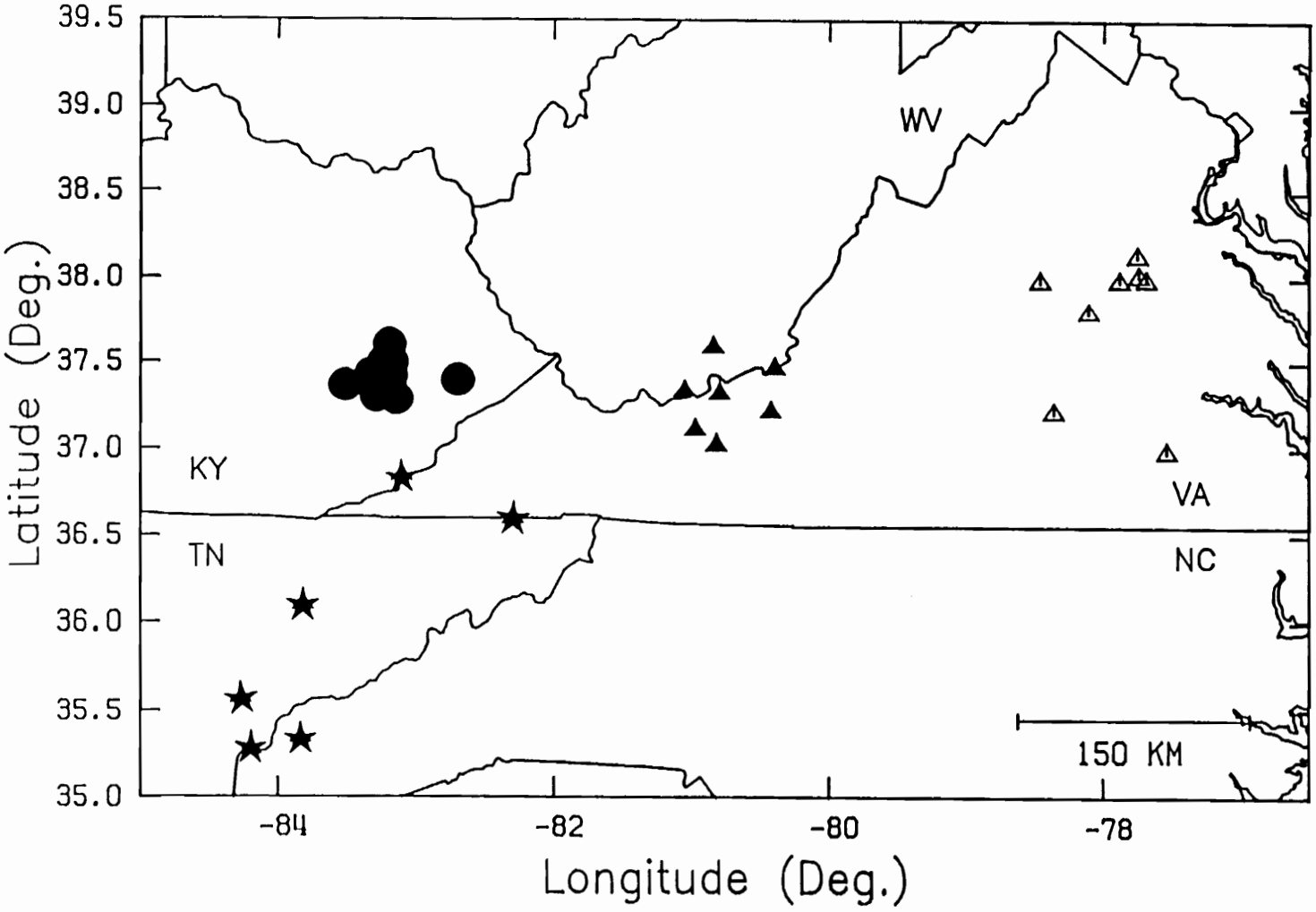

Figure 2. The Lg Q study area: VTSO stations indicated as in Figure 1. Regional earthquakes are shown as stars; blast sources are shown as solid circles.

Table 2. Epicentral data for events used in the RTSM analysis.

Event	Date (M-D-Y)	Source	Location (Deg)	Origin Time (UTC)	Distance (km)
861642054	06-13-86	Explosion	37.35N 83.51W	20h-53m-36.39s	240-500
870361638	02-05-87	Explosion	37.69N 78.33W	16h-38m-28.61s	35-221
880471527	02-16-88	Earthquake	36.60N 82.29W	15h-26m-54.8s	155-419

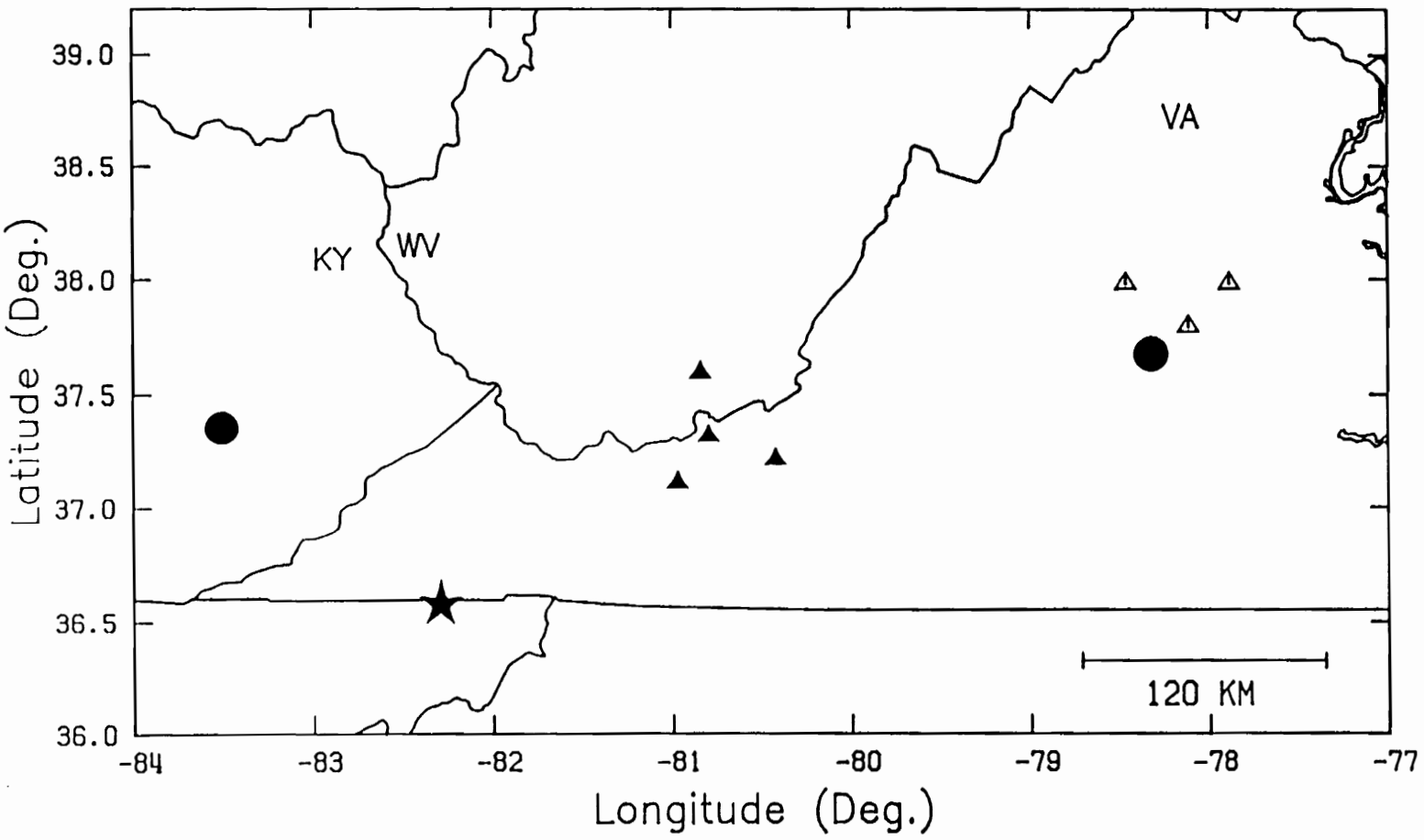

Figure 3. Sources and stations used in the RTSM study: VTSO stations indicated as in Figure 1. Earthquake source is shown as star; blast sources are shown as solid circles.

Table 3. Epicentral data for events used in coda Q analysis.

Event	Date (M-D-Y)	Location (Deg)	Depth (km)	Magnitude	Origin Time (UTC)	Lapse Times (sec)
860851635	03-26-86	37.25N 80.49W	12	2.9	16h-36m-23.9s	9.24-115.9
873250103	11-21-87	36.75N 80.70W	3	2.1	01h-03m-20.8s	21.8-66.8
873311859	11-27-87	36.85N 83.10W	15	3.5	18h-58m-29.5s	107.9-200.7
880471527	02-16-88	36.60N 82.29W	3.5	3.3	15h-26m-54.8s	75.62-123.12

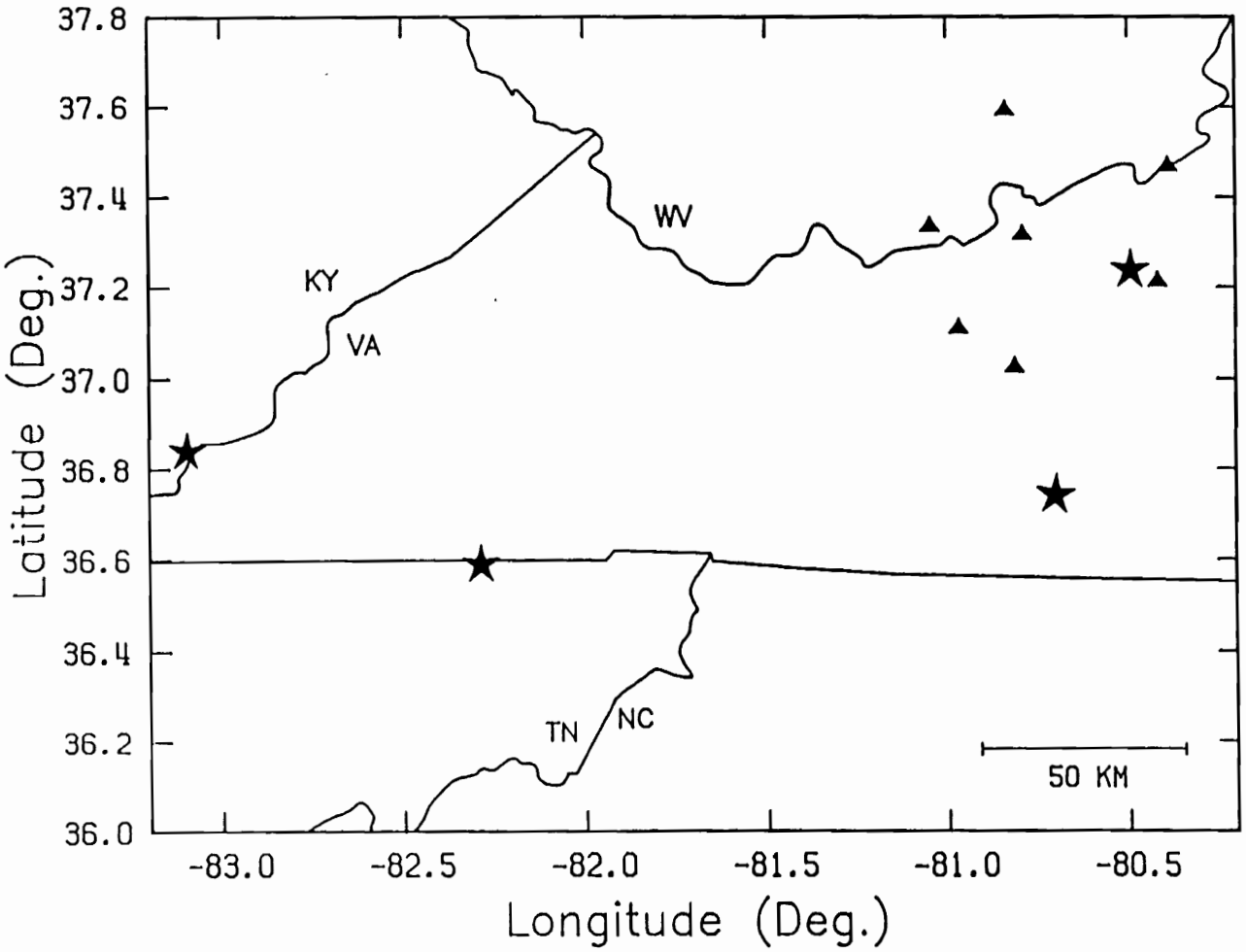

Figure 4. Coda Q study area: Stations and sources used in the coda Q study. Giles County subnetwork stations are shown as solid triangles; earthquakes are shown as stars.

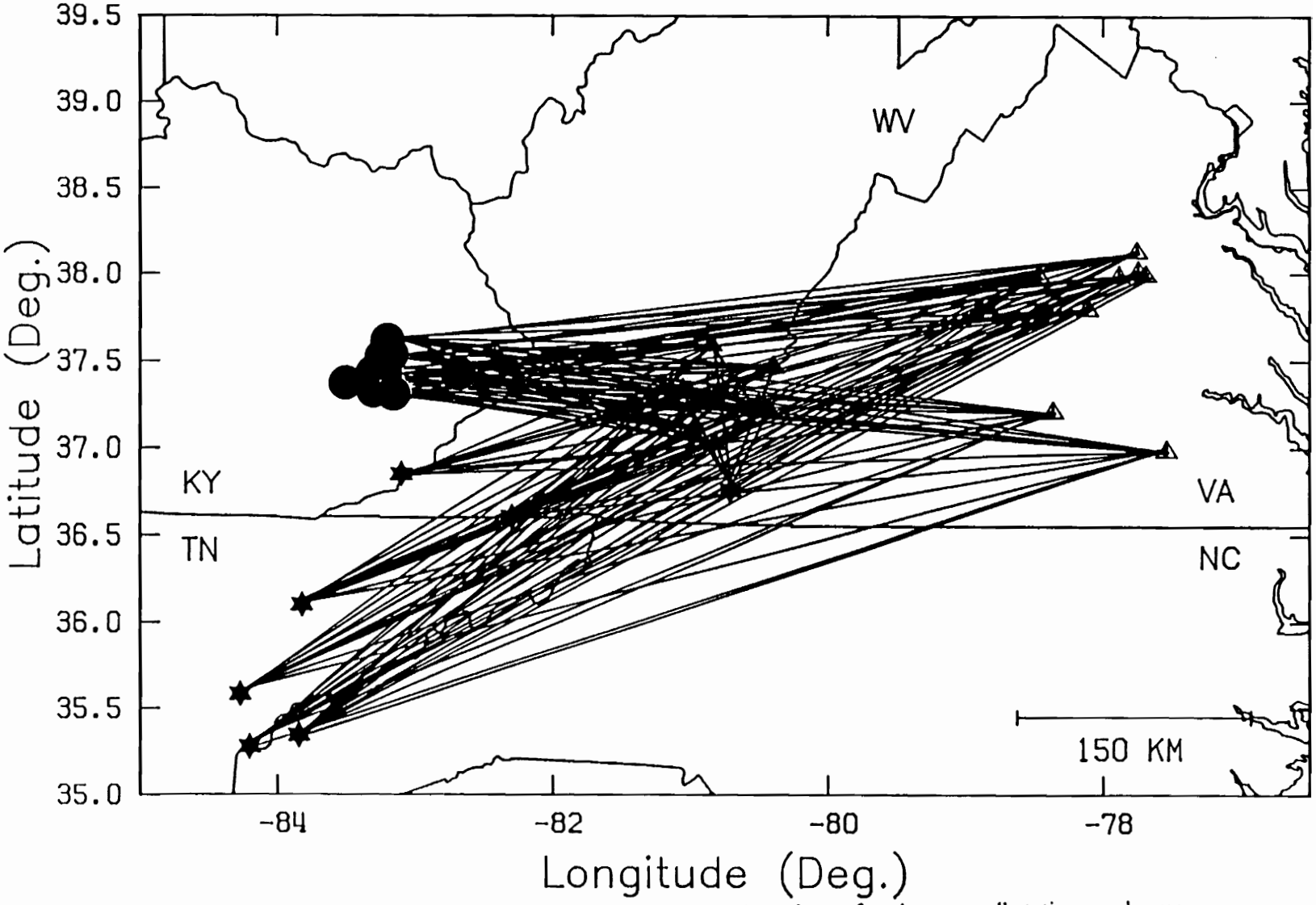

Figure 5. Area studied in Lg and coda Q analyses: Ray paths traced on the surface between all stations and sources in the Lg and coda studies.

in form, amplitude, period, and total duration (Tsujiura, 1978; Bollinger and Griffiths, 1979; King and Tucker, 1984; Tucker and others, 1984). Such studies have also shown that site responses are frequency dependent. These varying site effects should be considered when estimating the attenuation of ground motion in a region. A few of the seismic stations of the VTSO network are located on ridges and the network stations are located on a variety of geologic formations ranging from Precambrian metamorphics to upper Paleozoic sediments. There was concern, therefore, that site effects could be important in this attenuation study.

Two different site effect techniques were used in this study: 1) Relative station site responses were determined for several stations in the VTSO network from a calculation of mean residuals from the Q_{L_g} analysis. 2) The Reversed Two Station Method (RTSM) of Chun and others (1987) was used to obtain estimates of Q_{L_g} for Virginia and its environs that are free of site effect and instrument response problems. This was also done to determine whether other estimates of Q_{L_g} were contaminated by site effect problems.

Previous work

The assumption that Q_{L_g} and Q_C exhibit a power law frequency dependence: $Q_{(L_g,C)}(f) = Q_o f^N$ has been supported empirically in numerous studies (e.g., Lg waves: Campillo and others, 1985; Hasegawa, 1985; Chávez and Priestley, 1986; Chun and others, 1987; Coda waves: Rautian and Khalturin, 1978; Del Pezzo and others, 1983; Rodriguez and others, 1983; Pulli, 1984; Phillips and Aki, 1986). See Herraiz and Espinosa (1986) for a more complete list of Q_{L_g} and Q_C references. Values of Q_o and N vary among regions as shown in Table 4. For the continental United States, the variation may be summarized by the following averages of the regional values cited in Table 4, for frequencies in the range 1 to 10 Hz:

Q_{Lg}

Western U. S.	$Q_o = 303 \pm 235$	$N = 0.48 \pm 0.26$
Central U. S.	$Q_o = 855 \pm 912$	$N = 0.49 \pm 0.25$
Eastern U. S.	$Q_o = 1003 \pm 289$	$N = 0.39 \pm 0.25$

Q_C

Western U. S.	$Q_o = 220 \pm 69$	$N = 0.71 \pm 0.29$
Central U. S.	$Q_o = 673 \pm 569$	$N = 0.53 \pm 0.47$
Eastern U. S.	$Q_o = 500 \pm 332$	$N = 0.56 \pm 0.33$

In general, values of Q_o are less in the western United States than in the central and eastern U. S. This is expected, because studies of felt areas and isoseismal decay with distance have shown that attenuation of seismic waves is significantly greater in the western U. S. than in the east (Bollinger, 1973; Nuttli and Zollweg, 1974; Sibol and Bollinger, 1987).

Many attenuation studies have been done specifically in the eastern U. S. The results of those studies are presented in Table 5. A simple comparison of the values in Table 5 cannot be made. These studies have been done using several different analysis techniques and over various sized study areas. An inspection of the Q_C results in New England obtained by Pulli (1984) show how results can vary with study area size. He obtained values of $Q_o = 660$, $N = 0.4$ for all of New England ($\simeq$350,000 km^2) and $Q_o = 140$, $N = 0.95$ for southern New Hampshire and eastern Massachusetts only ($\simeq$40,000 km^2).

Regional geology

The seismic sources and the VTSO stations used in this study are located in the Appalachian mountains of Virginia, Kentucky, North Carolina, and Tennessee. This region is divided into four physiographic provinces which trend northeast - southwest: the Piedmont, the Blue Ridge, the Valley and Ridge, and the Appalachian plateau, see Figure 6.

Table 4. Worldwide variations of Lg Q and coda Q.

Location	Q_{Lg} (1 Hz)	N	Source Type	Reference
Canadian Shield	900	0.2	Earthquakes	Hasegawa (1985)
Central France	290	0.52	Earthquakes	Campillo and others (1985)
Great Basin	206	0.68	Nuclear Tests	Chávez and Priestley (1986)
Great Basin	214	0.54	Earthquakes	Chávez and Priestley (1986)
Great Basin	774	0.04	Earthquakes	Rogers and others (1987)
Basin and Range	220-345	0.2-0.4	Nuclear Test	Peseckis and Pomeroy (1984)
Basin and Range	139	0.6	Nuclear Tests	Nuttli (1986)
Southern California	200	0.7	Earthquakes	Nuttli (1981)
Central U. S.	1500	0.3	Earthquakes	Nuttli (1981)
Central U. S.	Q(1 Hz)	0.4	Earthquakes	Dwyer and others (1983)
Central MS Valley	210	0.78	Earthquakes	Dwyer and others (1984)

Location	Q_c (1 Hz)	N	Source Type	Reference
Southern Italy	Q(1 Hz)	0.45	Earthquakes	Del Pezzo and others (1983)
Basin and Range	250	0.45	Earthquakes	Singh and Herrmann (1983)
Great Basin	143	0.84	Earthquakes	Rogers and others (1987)
Great Basin	188	1.05	Nuclear Tests	Rogers and others (1987)
Western U. S.	200-400	0.4-0.6	Earthquakes	Singh (1981)
Baja California	37	0.87	Earthquakes	Rebollar and others (1985)
Petatlán, Mexico	47	0.87	Earthquakes	Rodriguez and others (1983)
Southeast Hawaii	65	0.44	Earthquakes	Huang and Wyss (1986)
Northwest Hawaii	72	0.46	Earthquakes	Huang and Wyss (1986)
Central MS Valley	270	0.87	Earthquakes	Dwyer and others (1984)
Central U. S.	800-1350	0.1-0.3	Earthquakes	Singh (1981)

Table 5. Eastern United States variations of Lg Q and coda Q.

Location	Q_{Lg} (1 Hz)	N	Source Type	Reference
Eastern U. S.	1000	0.35	Earthquakes	Goncz and Dean (1986)
Eastern U. S.	800	0.32	Earthquakes	Gupta and McLaughlin (1987)
Appalachians	1413	at 1 Hz	Earthquakes	Gupta and McLaughlin (1987)
Appalachians	1127	at 3 Hz	Earthquakes	Gupta and McLaughlin (1987)
Eastern U. S.	800	0.5	Earthquakes	Nuttli (1981)

Location	Q_c (1 Hz)	N	Source Type	Reference
S. Carolina	190	0.94	Earthquakes	Rhea (1984)
New England	140	0.95	Earthquakes	Pulli (1984) $t_i < 100$ sec
New England	660	0.4	Earthquakes	Pulli (1984) $t_i > 100$ sec
New England	460	0.40	Earthquakes	Pulli (1984) average t_i
Eastern U. S.	700-1000	0.3-0.4	Earthquakes	Singh (1981)

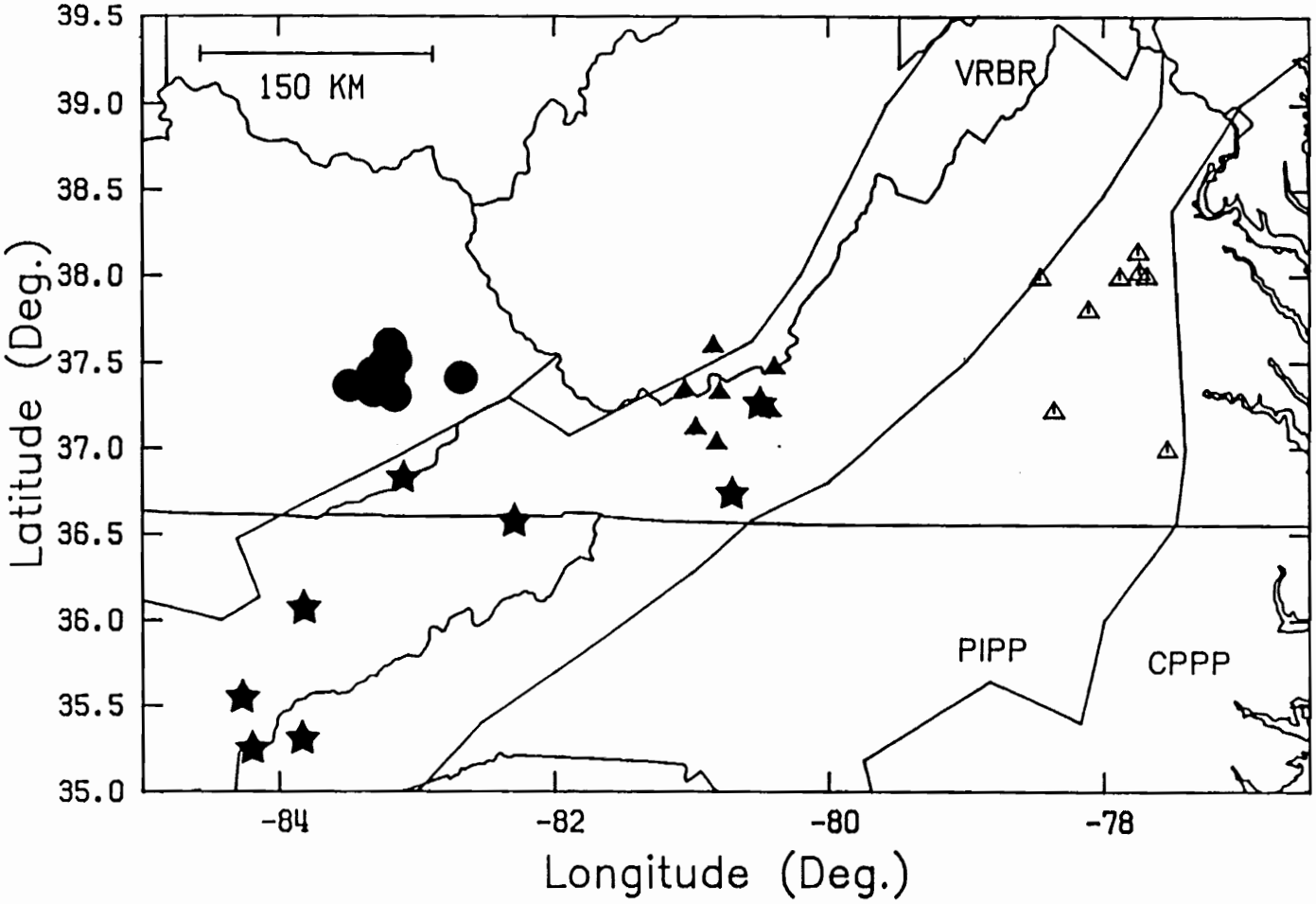

Figure 6. **Physiographic provinces of the Appalachian mountains:** CPPP - Coastal Plain province, PIPP - Piedmont province, VRBR - Valley and Ridge and Blue Ridge provinces. VTSO stations are shown as triangles; blast sources are located in the Appalachian plateau province and are shown as solid circles; earthquake sources are shown as stars.

The stations of the VTSO central Virginia subnetwork are located within the Piedmont. In general, the province is characterized by gently rolling terrain on belted crystalline rock which becomes increasingly hilly towards the mountains of the Blue Ridge province to the west. To the east the province is overlapped by the sediments of the Coastal Plain.

The western section of the Piedmont in Virginia consists of a group of pre-Middle Ordovician, Cambrian, and possibly older schists, quartzites, and metabasalts repeated in layers parallel to thrusting. East of this group are the Charlotte and Carolina Slate Belts which consist of higher grade metamorphic rocks of predominantly plutonic origin. These belts extend as basement rock under the Coastal Plain to the east (Hatcher and others, 1980; Glover and others, 1983).

The Blue Ridge province, a zone of rounded mountains 900 - 1800 meters high, is characterized by an approximately 2 - 3 km thick allochthonous sheet of highly metamorphosed Proterozoic and lower Paleozoic volcanic, sedimentary, and plutonic rocks. The metamorphic grade of the rocks increases to the east across this and the Piedmont province. A series of low angle thrust faults has been identified in the Blue Ridge. Large thrust blocks have been transported hundreds of kilometers along these faults which coalesce into a sole fault separating the thrust blocks from underlying relatively unmetamorphosed lower Paleozoic sediments. These sediments overlay crystalline basement rock. The northwestern border of the Blue Ridge, defined by the Blue Ridge fault, separates the highly metamorphosed Blue Ridge rocks from the folded and faulted but not otherwise highly deformed rocks of the Valley and Ridge province (Teague, 1984; Wehr and Glover, 1985; Pratt and others, 1987; Çoruh and others, 1988, in press, Geology).

West of the Blue Ridge fault, the Valley and Ridge in western Virginia and eastern Tennessee is a series of linear, level topped mountain ridges and narrow valleys eroded from sequences of Paleozoic sedimentary rocks. The sedimentary sequences are on the order of five kilometers thick and broken by eastward dipping imbricate thrusts which are related to a master décollement above the crystalline basement rock. The sedimentary rocks are unmetamorphosed, but exhibit folding and faulting which decreases in intensity westward towards the Appalachian plateaus (Harris, 1976; Hatcher and others, 1980; Teague, 1984; Wehr and Glover, 1985).

The north-westernmost sources used in this research are in eastern Kentucky, on the eastern edge of the Appalachian plateau. The youngest thrusts of the Appalachians are in the Valley and Ridge and displacements along these faults decrease to zero in the Appalachian plateau. The plateau marks the western extent of Appalachian style deformation and consists of approximately four kilometer thick relatively flat lying Paleozoic sedimentary rocks overlying the Grenville basement (Hatcher and others, 1980; Teague, 1984).

The thickness of the crust varies across this entire region. Under Giles County, the crust is considered to be approximately forty to fifty kilometers thick with P wave velocity increasing with depth from 5.6 to 6.5 km/sec. The S wave velocity varies with depth from 3.4 to 3.8 km/sec. Under central Virginia, in the Piedmont, the crustal thickness is approximately 36 kilometers with P wave velocities 6.1 to 6.5 km/sec and S wave velocities 3.5 to 3.8 km/sec (Bollinger and others, 1980).

Three areas of localized seismic activity are located in this region: the eastern Tennessee seismic zone, the Giles County seismic zone, and the central Virginia seismic zone. These are areas within the southeastern United States in which occur relatively large and more frequent earthquakes as compared to the majority of the region. The eastern Tennessee and Giles County seismic zones are located in the Valley and Ridge province. Earthquakes in these zones occur in the basement rock beneath the Appalachian décollement (hypocentral depths 5-25 km). The central Virginia seismic zone is located in the Piedmont province, with hypocenters above and along the Appalachian décollement (<13 km) (Bollinger and others, 1986; Çoruh and others, 1988 in press, Geology).

The Spectral Analysis of Q_{L_g} and Q_c

Lg spectral method

Amplitude spectra of Lg waves from regional earthquakes and blasts have been used to determine Q_{L_g} in various regions of the world (Campillo and others, 1985; Hasegawa, 1985; Chávez and Priestley, 1986), Table 4.

Chávez and Priestley (1986) model Lg amplitude spectra as

$$A(f,t,R) = \frac{S(f)}{R^{\nu}} e^{-\pi f t / Q_{L_g}(f)} \qquad [2]$$

where A is the spectral amplitude at a distance R, ν is a constant related to geometrical spreading, f is frequency (Hz), t is travel time, S is a source amplitude term, and Q_{L_g} is an attenuation term related to Lg decay. Q_{L_g} is a measure of intrinsic absorption and probably also measures attenuation by scattering. The model does not account for source radiation pattern, path, or site effects which may also affect the observed spectral amplitudes. A value of $\nu = 0.5$ is used for the geometrical spreading term in the frequency domain, assuming Lg to be a surface wave (see Appendix A).

To estimate Q_{L_g}, equation (2) is converted to a linear form by taking the common logarithm of both sides:

$$\log_{10}A(f,t,R) + 0.5\log_{10}R = \log_{10}S(f) - \frac{1.364ft}{Q_{Lg}(f)} \qquad [3]$$

where $1.364 = \pi \log_{10}e$. An estimate of Q_{L_g} at a particular frequency can be determined from the slope of ($\log_{10}A + 0.5\log_{10}R$) vs t plots for a seismic event ($Q_{L_g}(f) = \frac{\pi f \log e}{\text{slope}}$). The $t = 0$ intercept gives an estimate of source strength. Note, that because S(f) is common to all stations recording a given event, the source function has no influence on the estimate of Q_{L_g} if the radiation pattern can be assumed homogeneous. Any frequency dependence of Q_{L_g} can be examined by repeating the procedure using spectral amplitudes from an event at different frequencies. This method of Q_{L_g} determination requires at least one seismic source recorded at several stations. Data from several events in a region may be combined to obtain more concrete estimates of Q_{L_g}.

The assumed relationship between Q_{L_g} and frequency is of the form

$$Q_{Lg}(f) = Q_o f^N \qquad [4]$$

where $Q_{L_g}(f)$ is the quality factor for Lg waves at a frequency f and Q_o is Q_{L_g}(1 Hz).

Coda wave method

The decay of coda waves from local earthquakes is studied to determine the frequency dependence of Q_C for a study area. This measure of the quality factor includes both scattering and absorption effects, as is believed to be the case for Q_{L_g} as well. Herraiz and Espinosa (1986) provide an excellent summary of coda wave theory and recent research in the field.

A coda power spectrum can be separated into source and path terms: $P(f,t_i) = S^2(f)C(f,t_i)$ where $P(f,t_i)$ is the power spectrum of a coda wave at frequency f and lapse time t_i (time after origin time), $S^2(f)$ includes only source parameters, and $C(f,t_i)$ is a path term representing the effect of a large geographical area independent of epicentral distance and the details of the path connecting the source and station (Aki, 1969; Aki and Chouet, 1975). For this model, $C(f,t_i)$ is assumed to be

common to all sources and stations in a study area. A mathematical expression for $P(f,t_l)$ employing the single backscattering coda model takes into account geometrical spreading and attenuation due to anelasticity and scattering:

$$P(f,t_l) = \frac{S^2(f)}{t_l^a} e^{-2\pi f t_l / Q_c(f)}, \qquad [5]$$

where P is the power spectrum and S is a source amplitude term, t_l is lapse time (for body wave geometrical spreading $a = 2$; $a = 1$ for surface waves), and Q_C is the observed quality factor for coda waves including intrinsic absorption and scattering effects (Aki and Chouet, 1975). The power spectrum equation can be rewritten in linear form by the use of common logarithms:

$$\log_{10}(t_l^2 P(f,t_l)) = 2\log_{10} S(f) - \frac{2(1.364) f t_l}{Q_c(f)}. \qquad [6]$$

For this study, a relatively new spectral method of coda Q analysis was performed; spectral analysis of Q_C has been done by Rebollar and others (1985), Phillips and Aki (1986), and Fehler and others (1988). The method was suggested by M. C. Chapman (pers. comm.) and basically parallels the Lg spectral method. Power spectral amplitudes are determined for one seismic source at one station over successive time windows in the coda. An estimate of Q_C at a particular frequency can be determined from the slope of ($\log t^2 P$) vs. lapse time using the power calculated at one station in successive windows ($Q_C(f) = \frac{2\pi f \log e}{\text{slope}}$). Repeating this process for several frequencies, any frequency dependence of Q_C that may exist can be determined. Because Q_C is estimated from the coda power decay with time in successive time windows, only one source and one station are required for this analysis. The results from several stations and several events may be combined to obtain a better estimate of Q_C. As in the Q_{L_g} analysis, the assumed frequency dependence for Q_C is $Q_C(f) = Q_o f^N$.

Time domain analyses of coda wave decay are often performed using bandpass filtered seismograms of local earthquakes (Aki and Chouet, 1975; Pulli, 1984). Using the coda wave model

of Aki (1969) and Aki and Chouet (1975), the amplitude spectrum of the coda of a local earthquake is modeled as

$$A(f,t_l) = \frac{S(f)}{t_l^a} e^{\pi f t_l / Q_C(f)}$$

where A is amplitude, S is a source amplitude term, t_l is lapse time (for body wave spreading, a = 1), and Q_C is the observed quality factor for coda waves including anelastic attenuation and scattering effects.

For a bandpassed seismogram, the peak amplitude in successive time windows in the coda are determined for one seismic source at one station. An estimate of Q_C for the center frequency of the band considered can be determined from the slope of peak amplitude vs. lapse time plots ($Q_C(f) = \frac{\pi f \log e}{\text{slope}}$). Repeating this process for several different bandpassed seismograms, any frequency dependence of Q_C that may exist can be determined. The assumed frequency dependence of Q_C is $Q_C(f) = Q_o f^N$. Only one source and one station are required to obtain an estimate of Q_C. The results from several stations and several events may be combined to obtain a better estimate of Q_C.

Site Effects

Numerous studies have shown that seismograms of an earthquake recorded at stations on different geologic formations and in areas of large topographic relief differ significantly in form, amplitude, period, and total duration (Tsujiura, 1978; Bollinger and Griffiths, 1979; Tucker and others, 1984; King and Tucker, 1984). Such studies have also shown that site responses tend to be frequency dependent and weakly dependent on travel time, azimuth, and incidence angle of the input wave. Given that estimates of seismic source properties and attenuation are based on data recorded at various sites, it is clear that if varying site effects are not considered, any estimates made from amplitude measurements, including regional attenuation, may be in error.

Site response measurements

Measurements of site responses on different geologic formations have been made with fairly consistent results. Tsujiura (1978) studied the site responses of six stations in the Kanto district of Japan. The local surface geology of the station sites varied from loam and sandstone to crystalline schist and granite. He noted a correlation between site response factor and the site geology. Soft formations such as loam and sandstone had high site factors at low frequencies (0.75 Hz) and

smaller site factors at high frequencies (24.0 Hz). Hard formations such as granitic rocks showed smaller site factors at low frequencies and the greatest values at high frequencies.

Phillips and Aki (1986) discuss site amplifications at different frequencies calculated from data collected at California sites. At low frequencies (1.5 Hz), high site amplifications were associated with young sediments whereas low site amplifications were observed for stations on basement core complex rocks. At high frequencies (12.0 Hz), the site amplification pattern changed; the "well defined" low amplification of granite at low frequencies increased as frequency increased. Thus, their results agree with those of Tsujiura (1978).

Work in the Chusal Valley on the southern flank of the Tien Shan mountains by King and Tucker (1984) showed that site effects were virtually the same along the valley length where sediment thickness is approximately constant (40 - 60 m). Site effects varied by as much as a factor of five, however, between the valley middle and edge in studies crossing the valley width. The sediment layer across the width varies from 0 - 60 m in thickness. The factor of five site effect variation was seen in the 2 - 5 Hz range and appeared to be frequency dependent. Thus, the thickness of surficial formations appears to be relevant.

Bollinger and Griffiths (1979) investigated the effect of Appalachian topography on ground motion intensity in the study region. They placed 1 Hz horizontal and vertical seismometers on the tops and at the bases of ridges in the Valley and Ridge province in Virginia and Tennessee (average relief 300 m) and observed that ground motion on the mountain tops was amplified by a factor of 1.7 - 3.4 with respect to the adjacent valleys.

Site effect analysis

Because of the effect site responses have on the determination of various factors such as magnitude and regional attenuation, it is necessary to derive site correction schemes. Two methods are described here in which site responses are involved in the determination of attenuation parameters.

The Reversed Two Station Method (RTSM) of Chun and others (1987) is used to determine Lg attenuation. This method enables the determination of Q_{Lg} with site effects *removed* by using two stations and two events along a great circle path. The displacement spectral amplitude A is expressed as

$$A(f,d) = S(f)R(f,\theta)G(d)\Gamma(f,d)I(f)SS(f)$$

where f is frequency, d is epicentral distance, θ is station azimuth, and

$S(f)$ = source excitation function,

$R(f,\theta)$ = source radiation pattern term,

$G(d) = d^{-0.5}$ = Lg geometrical spreading term,

$\Gamma(f,d) = e^{-\alpha d}$ = anelastic attenuation term,

$\alpha = \frac{\pi f}{UQ_{Lg}(f)}$ = attenuation coefficient,

Q_{Lg} = quality factor for Lg waves,

U = group velocity,

$I(f)$ = assumed instrument response, and

$SS(f)$ = station site response.

The station site response is assumed to be independent of azimuth.

A particular configuration of stations and sources is necessary to use the RTSM. It is necessary that a pair of sources lie within a few degrees of a great circle path connecting two receivers located between the sources (see Figure 7). A product of spectral ratios (PR) is calculated (equation 7) and equated to a function that contains a generalized geometrical spreading term G_P and the attenuation factor α:

$$PR(f) = \frac{A(f,d_{2,far})A(f,d_{1,far})}{A(f,d_{2,near})A(f,d_{1,near})} \qquad [7]$$

$$PR(f) = G_P e^{-2\alpha(f)\Delta}. \qquad [8]$$

Or, after rearranging,

$$\alpha(f) = \frac{\log_{10} G_P - \log_{10} PR}{2\Delta \log_{10} e} \qquad [9]$$

where

$$G_P = \left(\frac{d_{1,far} d_{2,far}}{d_{1,near} d_{2,near}}\right)^{-0.5}. \qquad [10]$$

In the above equations, the subscripts 1 and 2 refer to seismic sources 1 and 2 on opposite ends of the great circle path. For each of the two sources, the subscript near refers to the closer recording station and far refers to the further station (see Figure 7). The interstation distance Δ is the mean of the two effective interstation distances associated with the two sources and two receivers.

The station site effects and instrument responses are not present in equation (9); these terms cancel in the spectral ratio multiplication in equation (7). The determination of α and, from that, Q_{L_g} becomes a relatively simple operation for any two pairs of stations and epicenters. To obtain regional estimates of Q_{L_g} this method is applied to a series of station - source combinations. Chun and others (1987) state that for interstation paths on the order of 100 km, no more than two or three combinations of data are needed to estimate Q_{L_g} because the results are highly repeatable. This is important for regions where network stations and regional seismic sources are not positioned along a great circle path.

Another approach to the site effect correction problem is to determine station site factors that can be used as correction terms in Q_{L_g} analysis. The Lg spectral amplitude A_{ij} at a station i from an earthquake j can be modeled as:

$$A_{ij}(f, t_{ij}, R_{ij}) = \frac{S_j(f)\ ST_i(f)}{R_{ij}^{0.5}} e^{-\pi f t_{ij}/Q_{L_g}(f)} \qquad [11]$$

where f is frequency, R_{ij} is epicentral distance, t_{ij} is travel time, S_j is a source amplitude term, ST_i is a station site response, and Q_{L_g} is the observed quality factor for Lg waves. Equation (11) can be rewritten in linear form as:

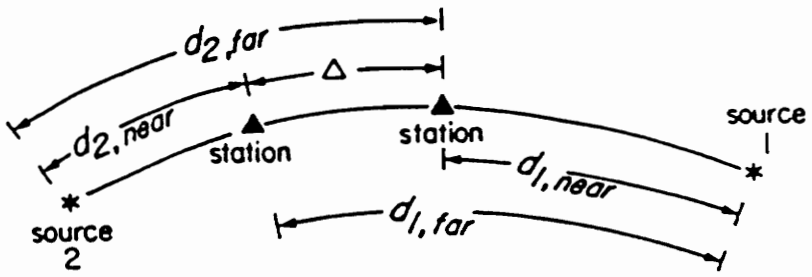

Figure 7. Station - source configuration for the Reversed Two Station Method: Schematic diagram of the source - station configuration necessary for application of the Reversed Two Station Method. To minimize radiation pattern effects the source - station azimuthal difference for station pairs must be small, $< 10°$. From Chun and others (1987).

$$\log_{10}A_{ij}(f,t_{ij}, R_{ij}) + 0.5\log_{10}R_{ij} - \log_{10}ST_i(f) = \log_{10}S_j(f) - \frac{1.364ft_{ij}}{Q_{Lg}(f)} \qquad [12]$$

The basic thesis of this model is that residuals from the Lg spectral analysis at a particular station and frequency are caused by station site effects. For various stations and the frequency band of interest (1-10 Hz here), Q_{L_g} is estimated as in the Lg spectral method from the slope of the observed values ($\log_{10}A_{ij} + 0.5\log_{10}R_{ij}$) vs t. It is assumed that $ST_i(f) = 1$ because the $\log_{10}ST_i(f)$ term in equation (12) goes to zero, as if no site effects were present. The residuals of this analysis for each station at each frequency are calculated. For a set of earthquakes, the mean of the residuals for a given station and frequency is considered the station site response. These station site responses may be used as site correction terms, the $\log_{10}ST_i(f)$ term in equation (12), in Q_{L_g} analyses performed using the same stations, but a different data set. This technique is analogous to that of Campillo and others (1985) who used a non-linear regression technique to simultaneously determine Q_{L_g} and site factors.

Data Analysis

All data analysis for this attenuation study was performed on the Virginia Tech Seismological Observatory (VTSO) PDP 11/34 and VAXstation II processors.

Q_{Lg}

Lg spectral method: The attenuation of the Lg phase (group velocity = 3.5 km/sec) in the Virginia area was studied from the short period vertical component digital recordings from VTSO network stations. The Lg spectral method discussed earlier in this paper was used. The sources used were ten regional surface mine explosions in the distance range 250 to 450 km and six regional earthquakes of magnitudes 3.3 to 4.2 in the distance range 150 to 650 km. The events used are listed in Table 1 and the locations are shown in Figure 2. A typical blast seismogram is shown in Figure 8.

The mine explosions were located using HYPOELLIPSE (Lahr, 1980) with the epicentral depths fixed at 0.01 km. The locations are not well enough constrained to identify specific coal mines: epicentral errors are approximately $\pm$ 10 km and the solution RMS values are in the range 0.2 - 0.6 seconds. The average azimuthal gap is approximately 330°. The locations and origin times

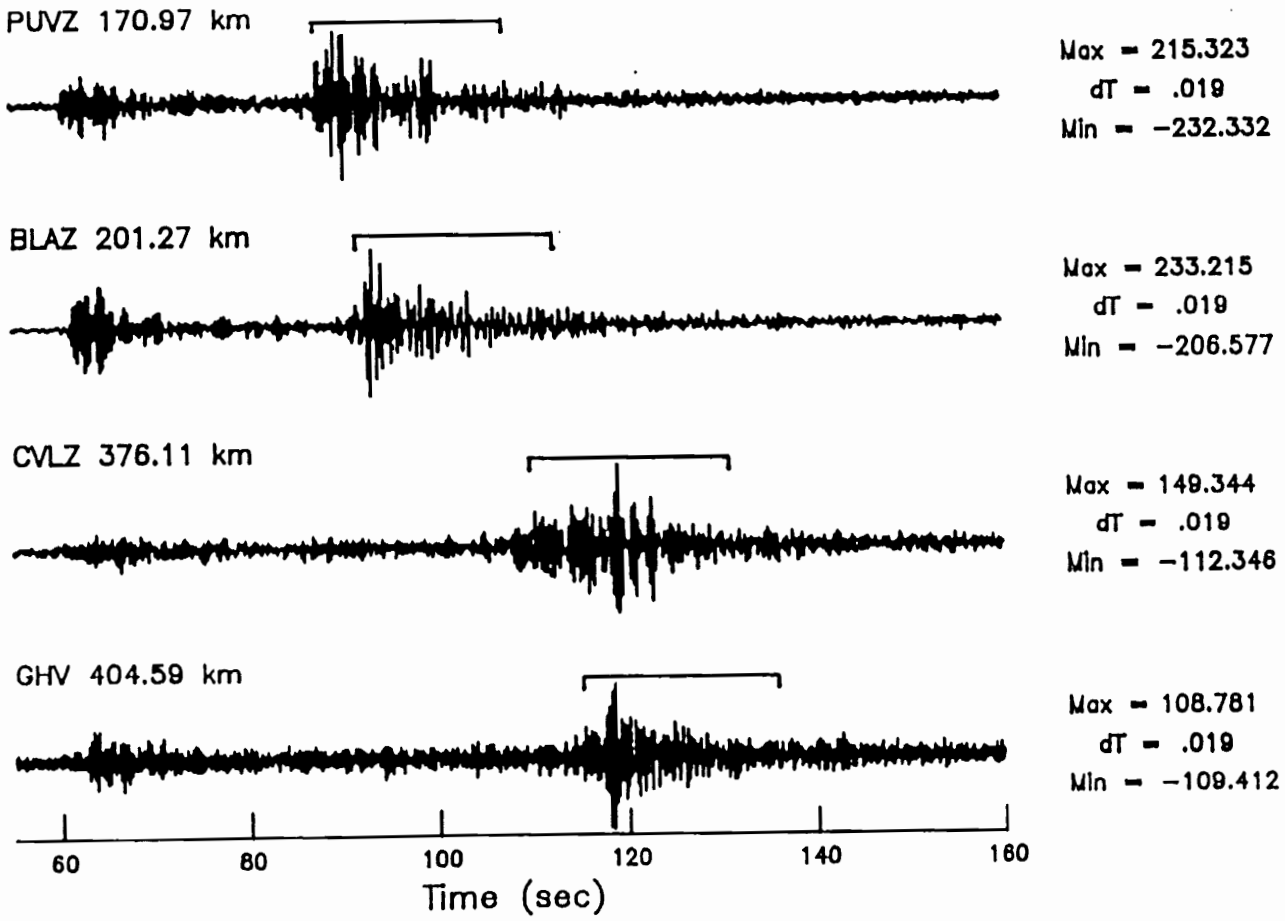

Figure 8. Typical seismogram from Lg Q analysis: Seismogram from an eastern Kentucky surface mine blast. Epicentral distance is indicated next to station name above trace; the Lg window studied is bracketed. Minimum and maximum amplitude values (relative scale) are indicated to the right of each trace, as is digitizing interval (dT = .019). Starting times have been adjusted so that P arrivals line up at 60.27 seconds.

of the regional earthquakes studied were obtained from U. S. Geological Survey Preliminary Determination of Epicenters lists and VTSO hypocentral locations.

Twenty second long Lg windows were used in the analysis. The beginning times of the windows were calculated from epicentral distances and origin times to coincide with the 3.5 km/sec arrival. Lg window start times were also determined visually from the arrival of the largest phase on the seismograms. These visual start times were consistently within 1 - 2 seconds of the calculated 3.5 km/sec arrival times; calculated start times were used for all spectral analysis.

The data at a station were deemed usable if the Lg spectral signal-to-noise ratio was at least four. This criterion limited the study to the frequency band 1 - 10 Hz and, in the case of some events, to narrower bands ($\simeq 1 - 6$ Hz). The noise spectra used in the signal-to-noise ratios were also derived using twenty second windows. Two noise windows were used, one preceding the P wave arrival and one following the signal coda, Figure 9. Individual stations with low (< 4) signal-to-noise ratios in the band 1 - 10 Hz were deleted from the Q_{L_g} analysis, as were entire events if the signal-to-noise ratio for a majority of the stations across the network was not at least four. A Hanning taper was applied to the time windows before the Fourier transforms were calculated and all stations were instrument corrected. Several other window types were tested (boxcar, five percent cosine, and Hamming). No appreciable differences in the spectra or the final Q_{L_g} estimates were observed for the various windows. The Hanning window was used because it generated smooth spectra and has been used in other similar studies (Hasegawa, 1985; Phillips and Aki, 1986). The results of the window testing are presented in Appendix C.

An additional test of the data was a comparison of amplitude spectra, Figure 10. For an individual event, significant deviations of station spectra from the general subnetwork trend were considered the probable result of local site effects or incorrect station calibration. Data at such stations were removed from analysis. The spectra plots from the two VTSO subnetworks were also compared to obtain a general idea of the amplitude decay with distance, Figure 11. Events for which the spectral decay across the network was judged to be inadequate were not used. The lack of noticeable amplitude decay was considered the probable result of low signal-to-noise ratio, site effects, and/or incorrect station calibration.

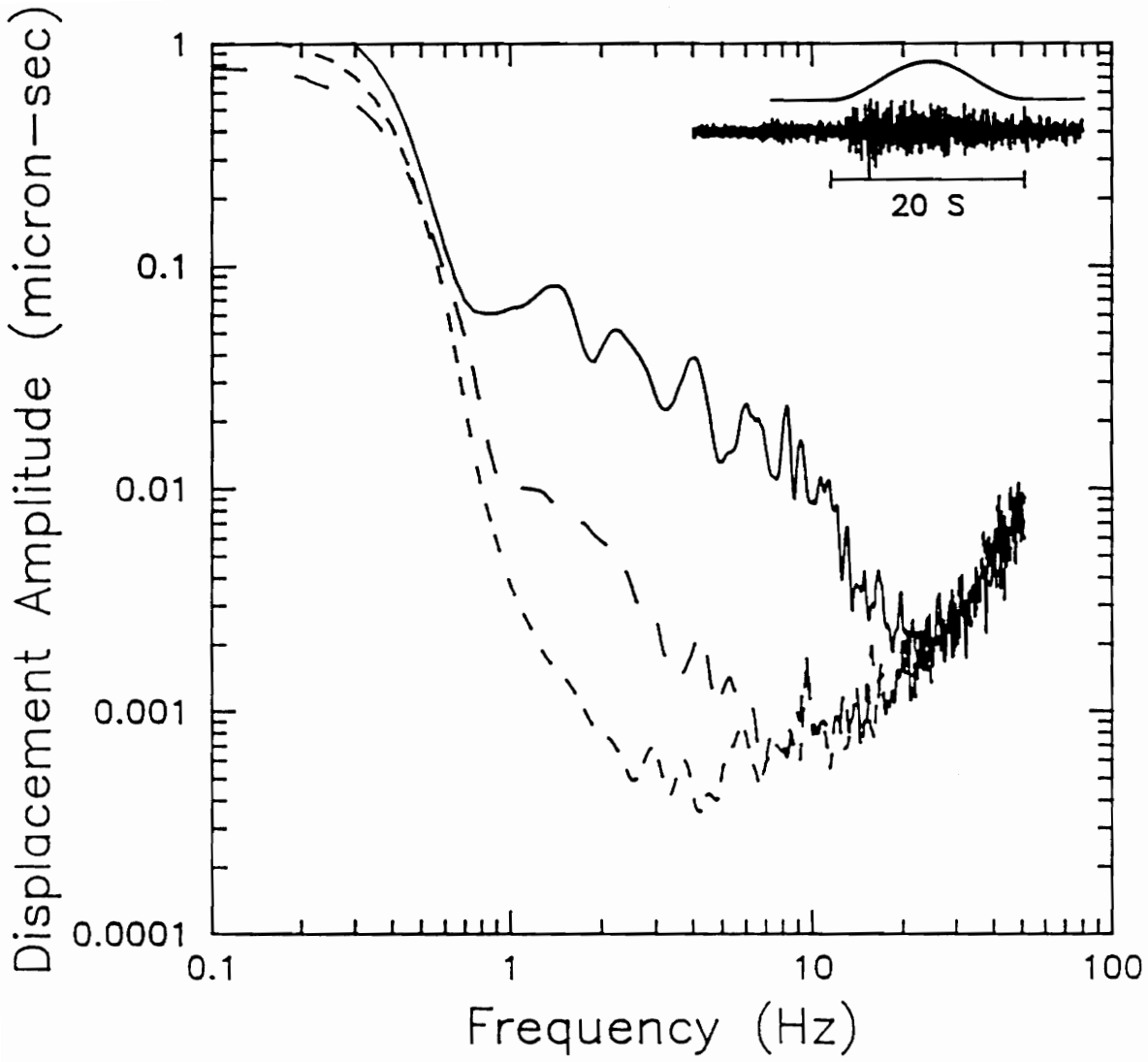

Figure 9. Signal and noise spectra for a typical Lg event: Lg spectrum plotted as solid line, noise spectra from before P arrival and after Lg coda plotted as dashed lines. Lg signal window and Hanning taper are indicated in the upper right corner. All spectra are smoothed using a modified Daniel smoothing technique before being plotted.

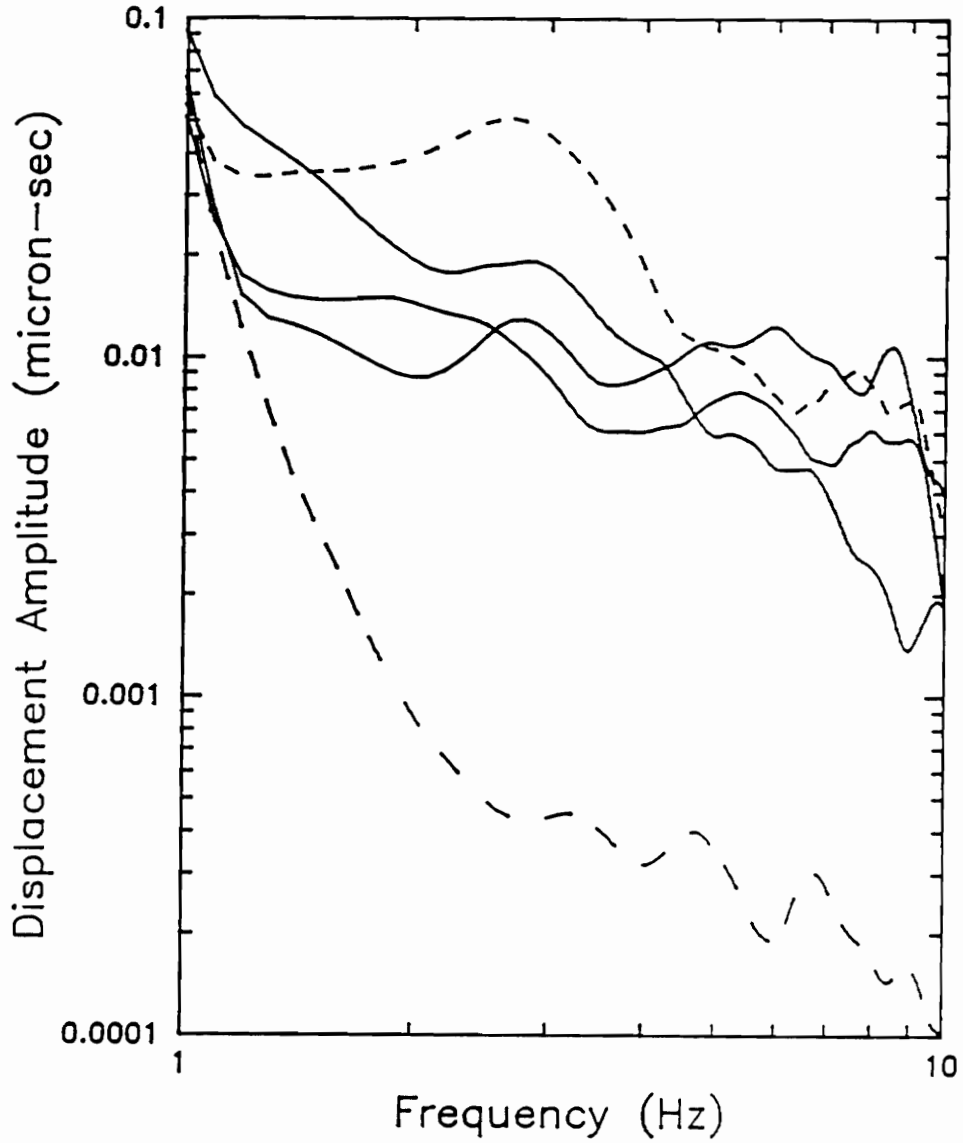

Figure 10. Lg spectra of an event from Central Virginia stations: Significant deviations from the general spectra trend such as the short dashed line were considered the result of local site effects and/or incorrect station calibration and these data were removed from analysis. A representative noise spectrum is shown by the long dashed line. All spectra are smoothed using a modified Daniel smoothing technique before being plotted.

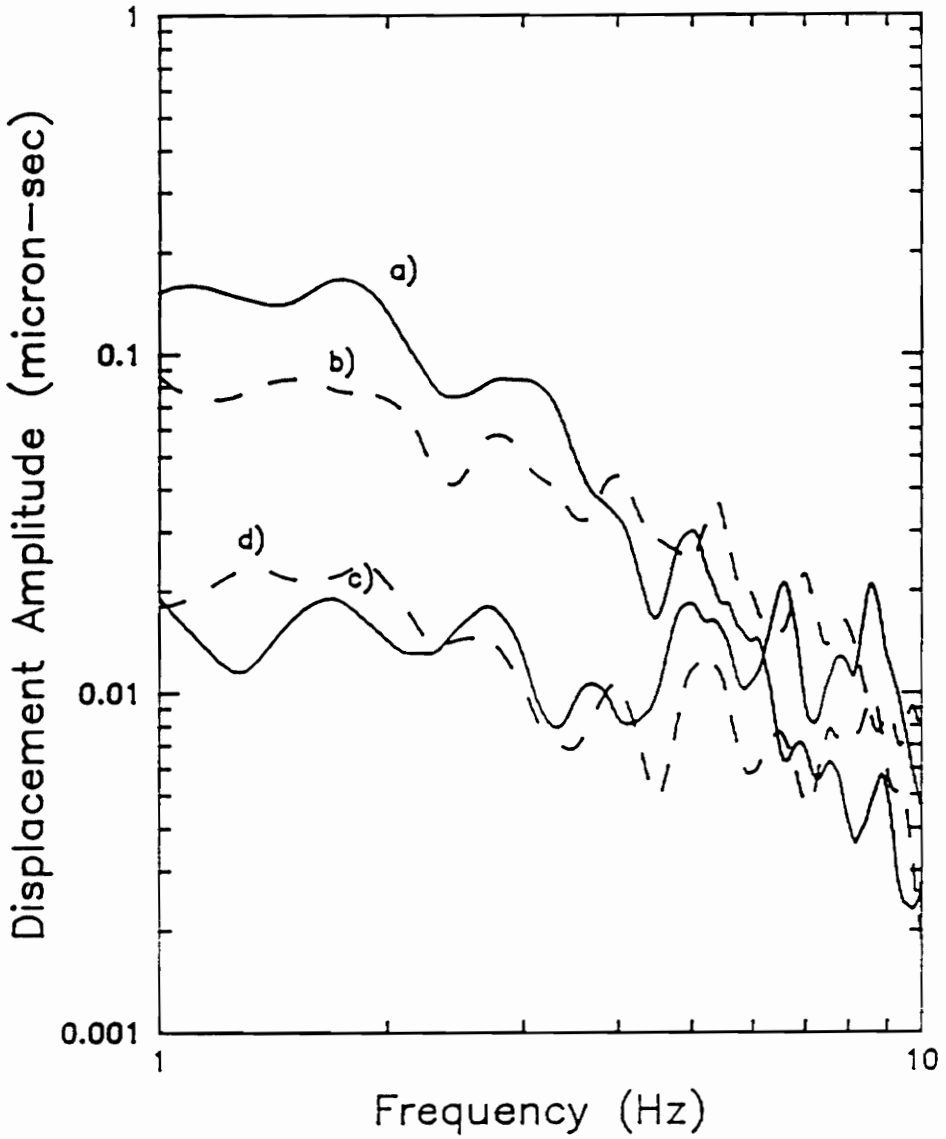

Figure 11. Lg spectra of an event at various distances: Lg spectra of an event from various stations across the VTSO network. Note that spectra converge and at times cross at higher frequencies. All spectra are smoothed using a modified Daniel smoothing technique before being plotted. Noise level is as in Figure 10. a) and b) Giles County stations 140-180 km, c) and d) Central Virginia stations 425-431 km.

When an event met the signal-to-noise and spectra trend criteria, analysis to estimate Q_{Lg} for various frequencies was performed. Because of the random character of the signal amplitude spectra, an objective smoothing method is desirable. The logarithmic mean of the amplitude spectra for each event was calculated in five octave frequency bands centered at 1.5, 3.0, 6.0, 9.0, and 12.0 Hz and the mean value was assigned to the center frequencies. The results obtained using the mean spectra in frequency bands were equivalent to those obtained using continuous frequencies within the 1 to 10 Hz band. These spectral amplitudes were corrected for geometrical spreading as in equation (3) and values of ($\log_{10}A + 0.5 \log_{10}R$) vs t were calculated at a given frequency, Figure 12. This process was performed using various stations recording a seismic event and repeated for the five frequency bands considered. The correlation coefficients (R^2) of these plots were used as a basis for editing out inaccurate data. For further analysis, no amplitude decay data with $R^2 < 0.5$ were used. This process was repeated for the ten blasts and six earthquakes studied. Q_{Lg} and frequency data from the above plots were used to estimate the frequency dependence of Q_{Lg}, assuming the form $Q_{Lg}(f) = Q_o f^N$. Estimates were made for all the earthquake data, all the blast data, and the two data sets combined using amplitude decay data with correlation coefficients greater than 0.5, 0.7, and 0.8. These results are presented in the *Results* section and serve as a basis for comparison of $Q_{Lg}(f)$ from earthquake data and from explosion data and for comparison of Q_{Lg} and Q_C results in the *Discussion* section of this paper.

RTSM: The Reversed Two Station Method (RTSM) of Chun and others (1987) was also used to estimate Q_{Lg} in the crust of the Virginia area. This method was used to determine Q_{Lg} with the effect of station site factors removed. If the results obtained with this method agree with those of the Lg spectral method, we can increase our confidence that our qualitative removal of inaccurate data based on a spectral comparison has succeeded in removing data at stations with questionable site effects or instrument response corrections.

Because of the station - source configuration involved in the RTSM, it was necessary to find sources in central and eastern Virginia. An unusually large quarry explosion in central Virginia was

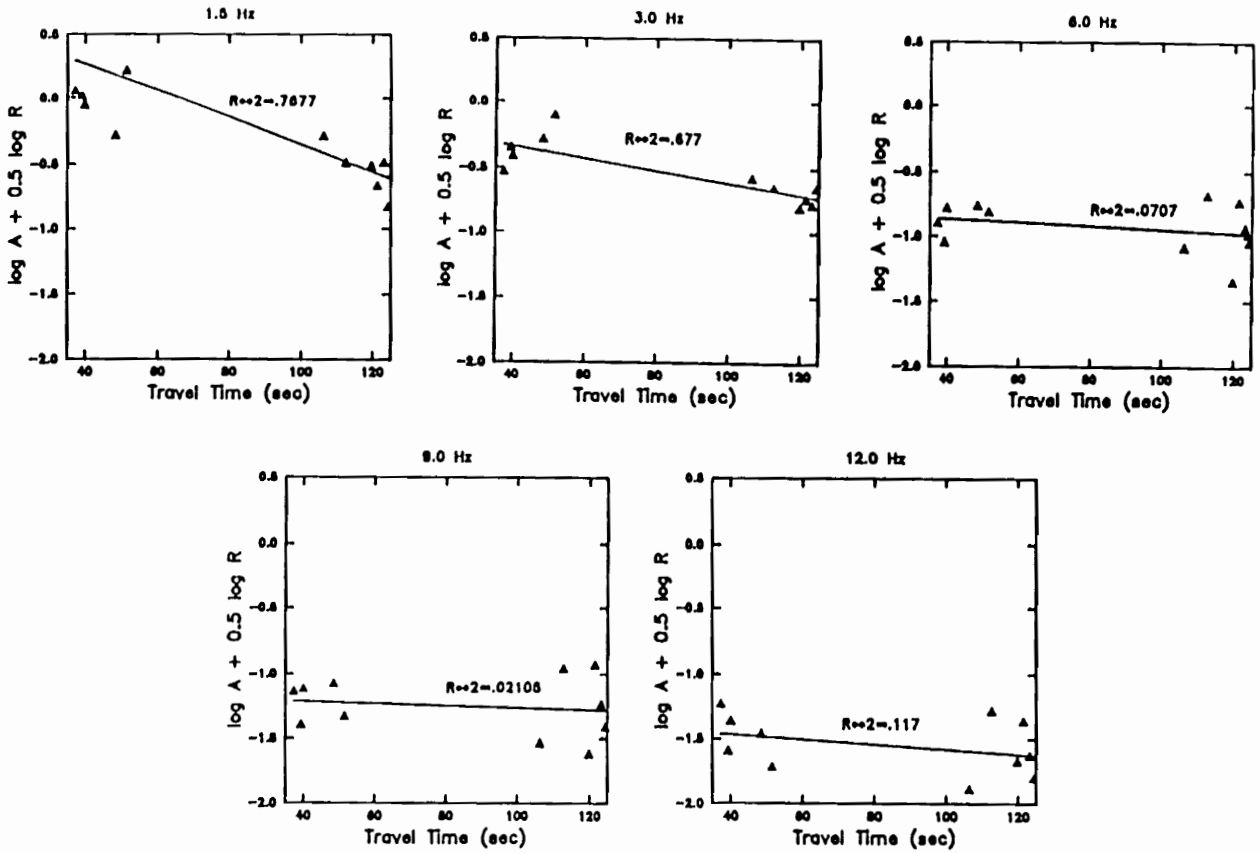

Figure 12. (log A + 0.5 log R) vs t: Plots of corrected amplitude decay with increasing travel time for an event. The slope is related to Q_{Lg}, t = 0 intercept is a measure of source strength.

found in an appropriate location to be paired with a representative eastern Kentucky coal mine explosion and a southwest Virginia earthquake (Figure 3, Table 2).

Signal-to-noise ratios were determined for the blast at the stations to be used. This was done as in the Lg spectral method. Ten second time windows were analyzed because the signal from this locally recorded blast was shorter in duration than those from the earthquakes and regional blasts used in the Lg spectral method. For each source - station grouping used, the Lg amplitude spectra were calculated for each source at both stations. As in the Lg spectral analysis, the amplitude spectra were calculated in five octave frequency bands with center frequencies 1.5, 3.0, 6.0, 9.0, and 12.0 Hz.

The station - source distances and spectral amplitudes were used to calculate Q_{L_g} from a ratio of spectral products as discussed in the *Site Effects* section of this paper. Several sets of source - station groupings were analyzed to obtain site effect free estimates of Q_{L_g} for the crust in the Virginia area. These esults are presented in the following *Results* section.

Site effect correction terms: The residual site response correction method discussed in the *Site Effects* section was used to identify station site responses. The complete Lg data set was processed using the Lg spectral method. The residuals for each station in each frequency band were calculated. For the j events studied, the mean of the residuals at one station (of a total of i stations) and one frequency, i.e., $\sum_{n=1}^{j} ST_i(f)/j$, was called the station site response. These responses may be used as site correction terms in future, more extensive Q_{L_g} studies. The application of these correction terms to the data set used to derive them is not considered appropriate. The mean station responses for one station in the five frequency bands are shown in Figure 13. Other station response estimates are listed in Appendix D.

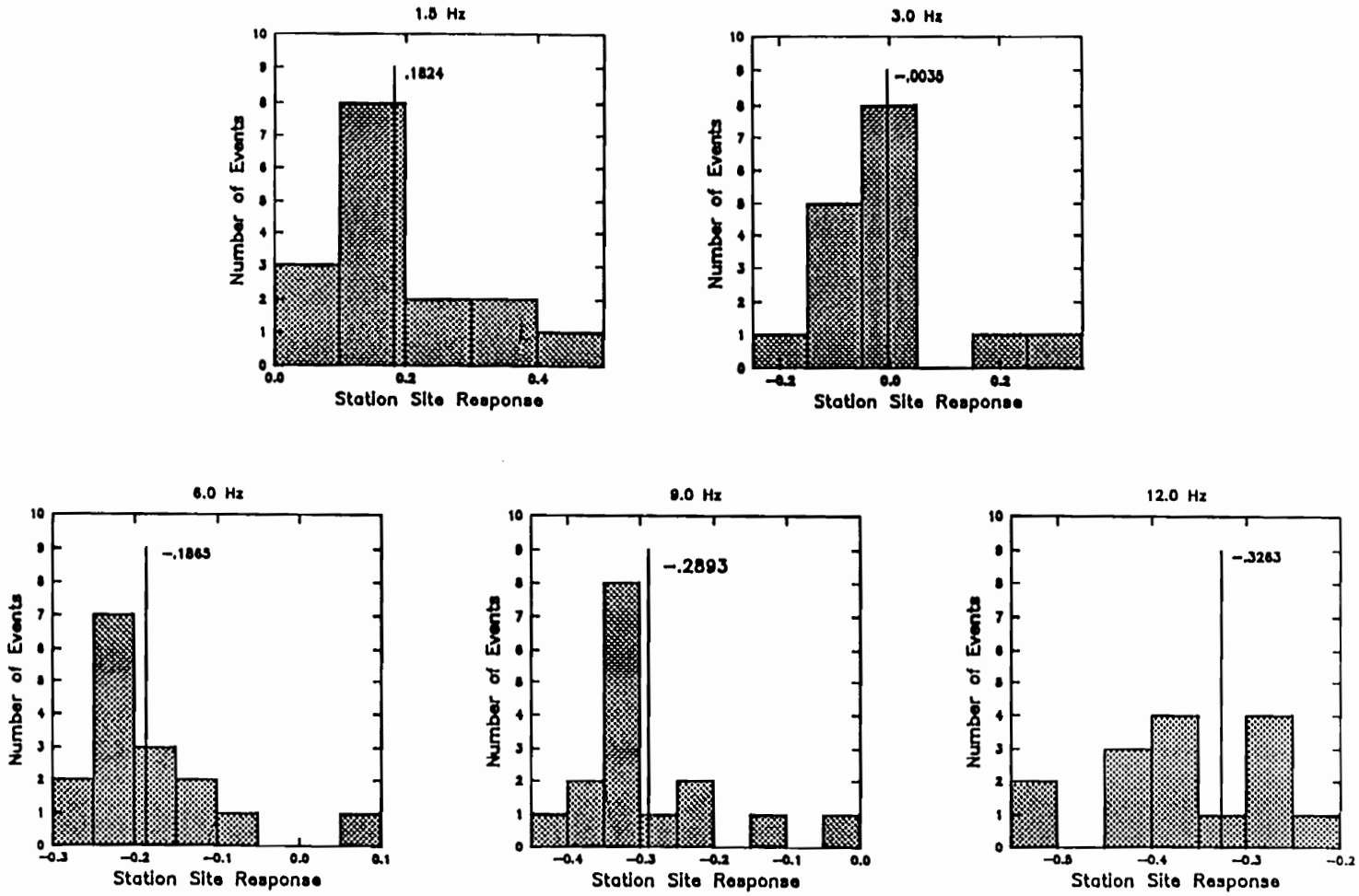

Figure 13. Station site responses for VTSO station BLAZ: Mean station site responses for five frequency bands calculated from a set of 16 events. Distribution of the responses shown by shaded bars; mean station site response shown by solid lines with adjacent numerical values.

Q_c

The decay of the S wave coda in western Virginia was studied according to the single scattering model of Aki and Chouet (1975). Estimates of Q_C were derived from the temporal decay of coda power spectra within the Giles County, Virginia VTSO subnetwork. Four local earthquakes were used in this study in the magnitude range 2.1 to 3.2 and distance range 6 to 260 km (Figure 4, Figure 14, and Table 3).

According to the coda wave method the power spectrum of an earthquake was calculated at each recording Giles County station. The logarithmic mean of the coda power spectra was calculated in each of five octave wide frequency bands centered at 1.5, 3.0, 6.0, 9.0, and 12.0 Hz. The mean power in each window was assigned to the band center frequency. The power spectra at each station were calculated in successive, non-overlapping five second windows beginning at a time equal to Origin Time + (2 × S wave travel time). The power in successive windows was calculated until the signal-to-noise ratio was less than four for any one of the frequency bands. A ten second noise window preceding the P wave arrival was analyzed to establish the noise power, Figure 15. As in the Lg spectral analysis, all time windows studied were Hanning tapered and all stations were instrument corrected. The spectral power amplitudes were corrected for geometrical spreading as in equation (6) and values of ($\log_{10} t_i^2 P$) vs lapse time were calculated at a given frequency, Figure 16. The correlation coefficients (R^2) of these plots were used as a basis for editing out inaccurate data. For further analysis, no power decay data with $R^2 < 0.5$ were used.

This process was performed using the power data from successive time windows of the coda at one station and repeated for the five frequency bands considered. This process was repeated for all Giles County stations recording each of the four local earthquakes. For each earthquake, Q_C and frequency data obtained from the above plots were used to estimate the frequency dependence of Q_C, assuming $Q_C(f) = Q_o f^N$. The data for all four earthquakes were then combined for a composite $Q_C(f)$ estimate. These values are presented in the *Results* section and are compared with Q_{Lg} results in the *Discussion* section of this paper.

To test the validity of the spectral method used here, values of Q_C in the five frequency bands were determined using a time domain analysis method as discussed earlier. The temporal decay of peak amplitudes was estimated using bandpassed seismograms of one local earthquake as recorded at four Giles County stations. Decay envelops were visually fitted to the peak amplitudes of the bandpassed seismograms. Successive, non-overlapping five second windows beginning with time equal to Origin Time + (2 × S wave travel time) were marked. Envelop-to-envelop measurements (equal to 2A) were made at the center of each window until the signal-to-noise ratio was less than four (the same limit as in the frequency domain measurements). A least squares fit was made to the amplitude (A) versus lapse time (t_l) data. Values of Q_C were obtained from the slope of the linear fit ($Q_C(f) = \frac{\pi f \log e}{\text{slope}}$). The results for the five frequency bands were combined for each of the four stations, assuming $Q_C(f) = Q_o f^N$. The results for the four stations were then combined for an estimate of Q_C for the one earthquake studied. The values obtained are presented in the *Results* section and are compared with the frequency domain Q_C results in the *Discussion* section of this paper.

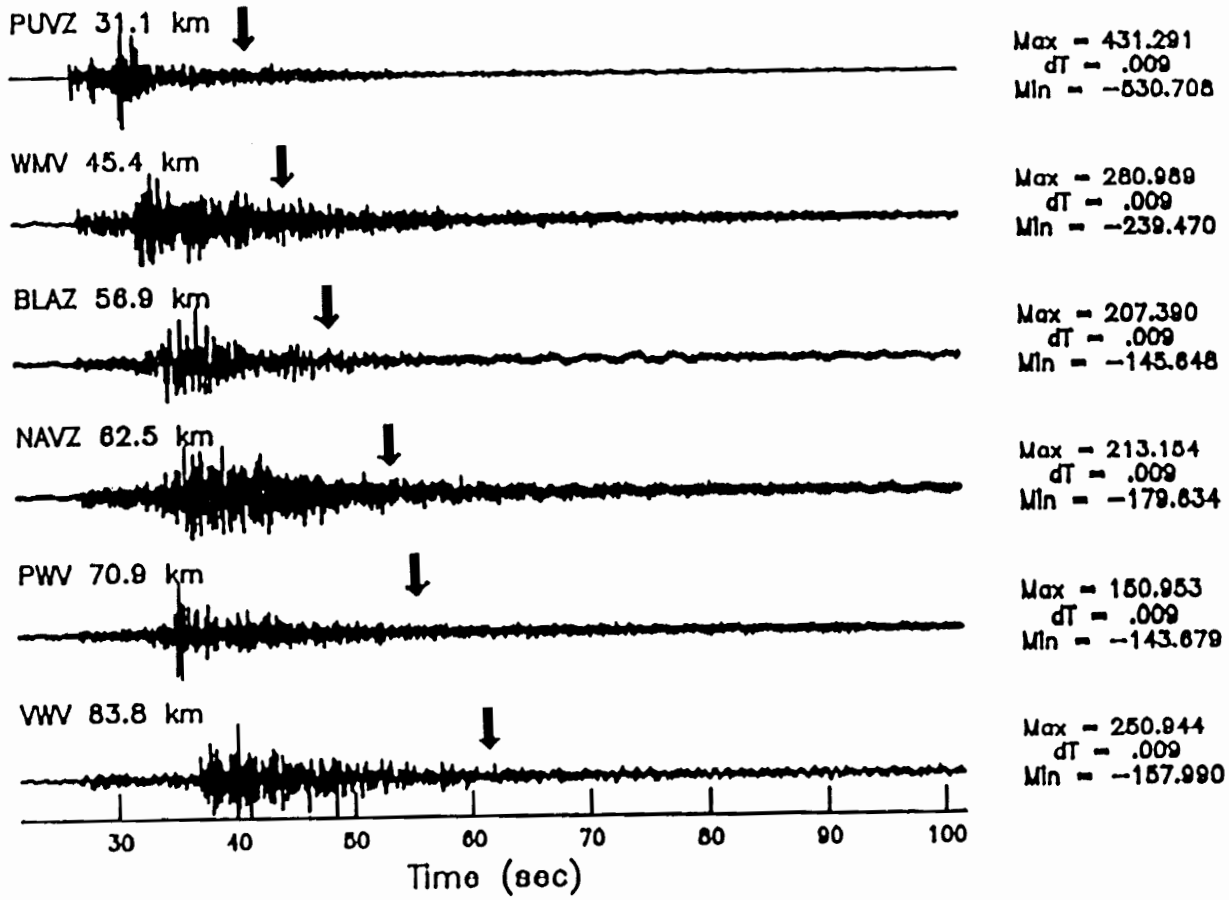

Figure 14. Typical seismograms from coda Q analysis: Seismogram from a local earthquake. Epicentral distance is indicated next to station name above trace. Beginning time for windowing indicated by an arrow. Minimum and maximum amplitude values (relative scale) are indicated to the right of each trace as is the digitizing interval (dT = .0098). Starting times have been adjusted so that P arrivals line up at 26.67 seconds.

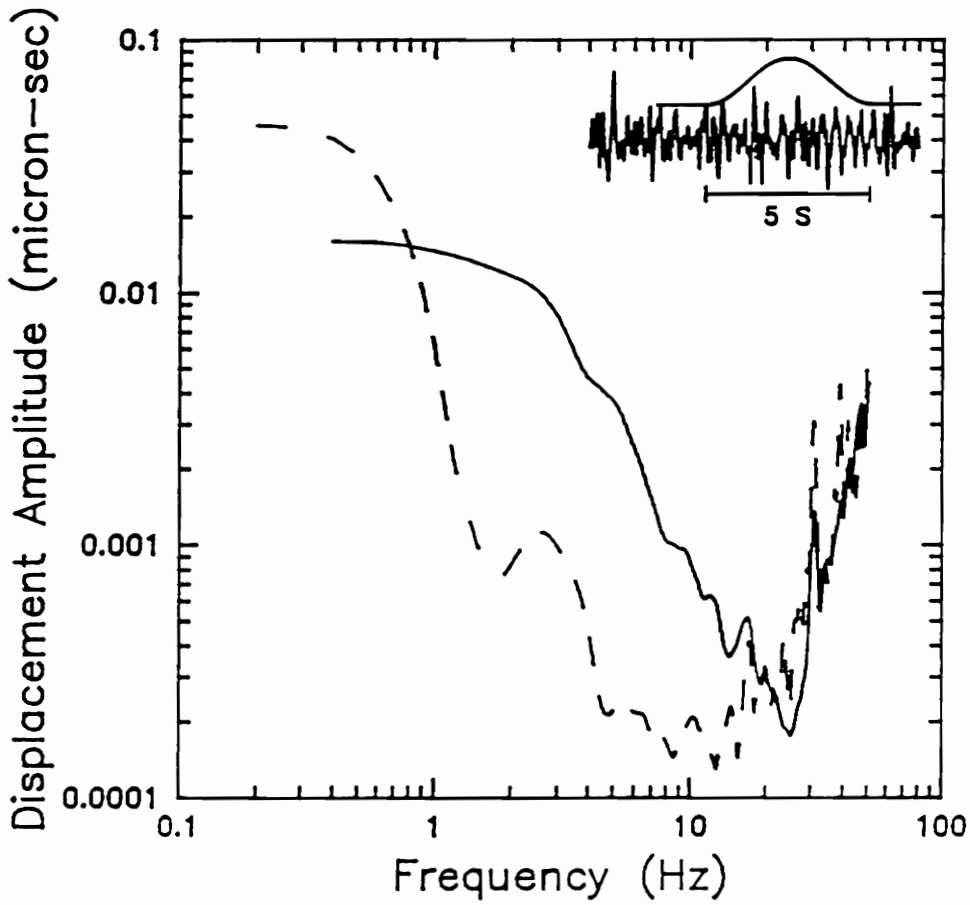

Figure 15. Signal and noise spectra for a typical coda event: Coda amplitude spectrum plotted as a solid line, noise spectrum from before P arrival plotted as dashed line. Coda window and Hanning taper are indicated in the upper right corner. All spectra are smoothed using a modified Daniel smoothing technique before being plotted.

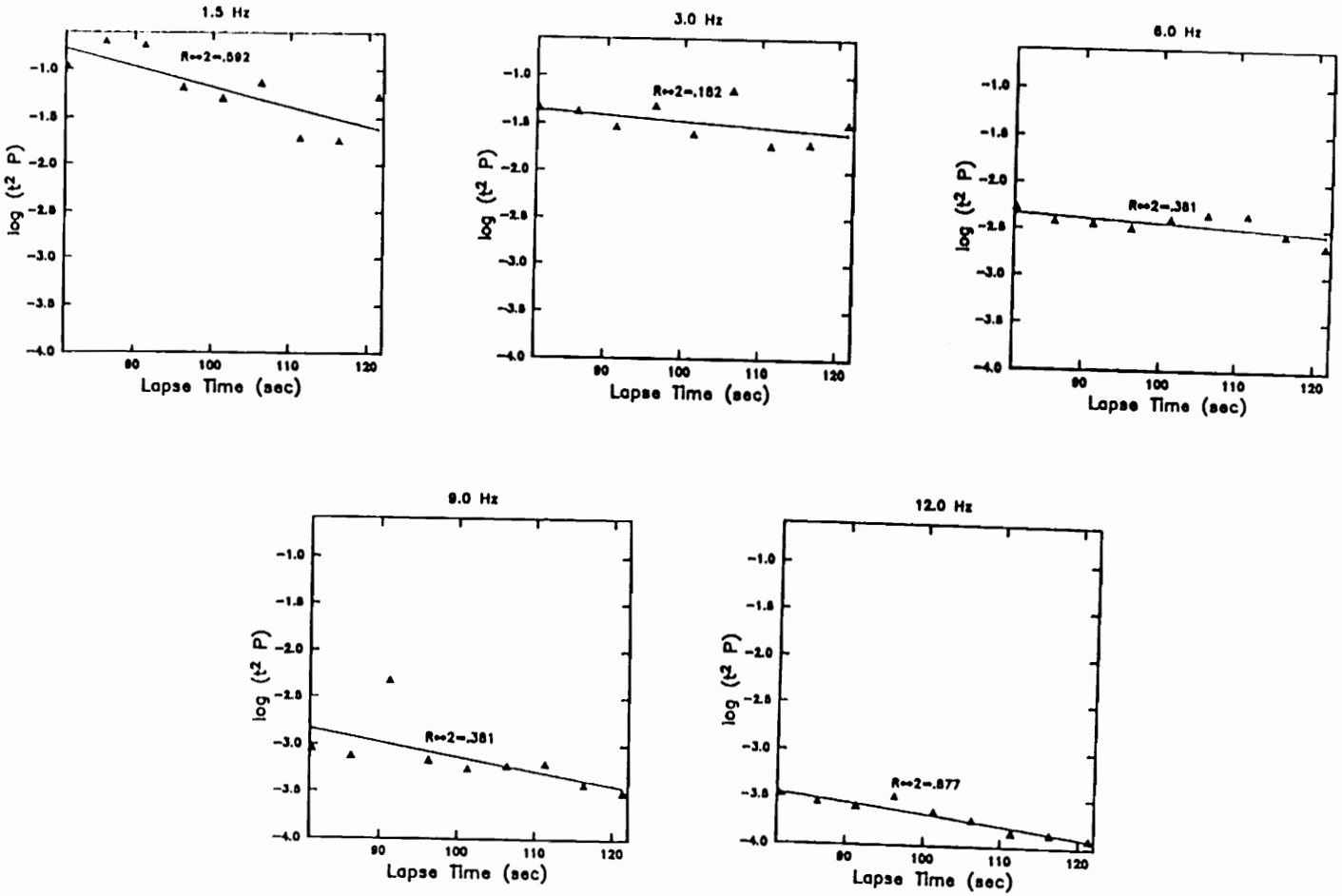

Figure 16. (log t^2 P) vs t: Plots of corrected coda power decay with lapse time for one station and one source.

Results

Q_{Lg}

The Lg spectral analysis method was used to estimate Q_{Lg} in the crust of the Virginia area. Q_{Lg} was estimated from the decay of Lg spectral amplitudes across the Virginia Tech Seismological Observatory (VTSO) digital network and was determined to be frequency dependent: $Q_{Lg}(f) = Q_o f^N$. The analysis was performed on three sets of data: ten regional surface mine explosions (epicentral distance range 250 - 450 km), six regional earthquakes (distance range 150 - 650 km, magnitudes 3.3 - 4.2, focal depths 5 - 26 km), and the blast and earthquake data combined.

For the frequency range 1 - 4 Hz, the results of the Q_{Lg} analysis are shown in Figure 17 and can be represented by:

Explosion data	$Q_o = 190$	$\sigma_{\log Q_o} = 0.06$	$N = 1.1 \pm 0.15$
Earthquake data	$Q_o = 149$	$\sigma_{\log Q_o} = 0.05$	$N = 1.5 \pm 0.15$
Combined data	$Q_o = 186$	$\sigma_{\log Q_o} = 0.05$	$N = 1.1 \pm 0.1.$

The individual data points shown in Figure 17 represent data from ($\log_{10}A + 0.5 \log_{10}R$) vs t plots with correlation coefficients greater than 0.7 (earthquake data) and 0.8 (explosion and combined data).

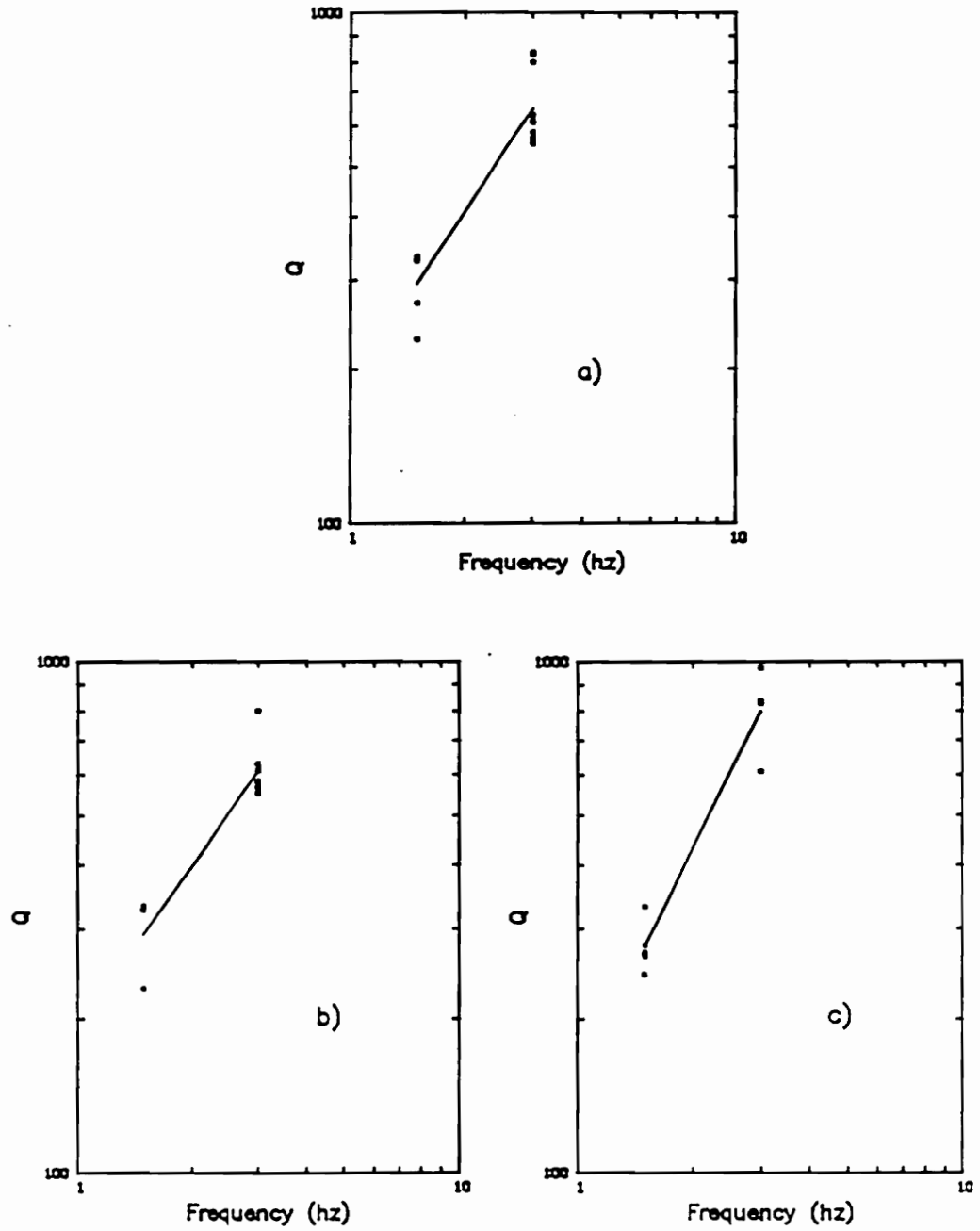

Figure 17. Q_{Lg} results from the Lg spectral method: Results from Lg spectral method for western and central Virginia: a) combined earthquake and explosion data, b) explosion data set results, and c) earthquake data set results.

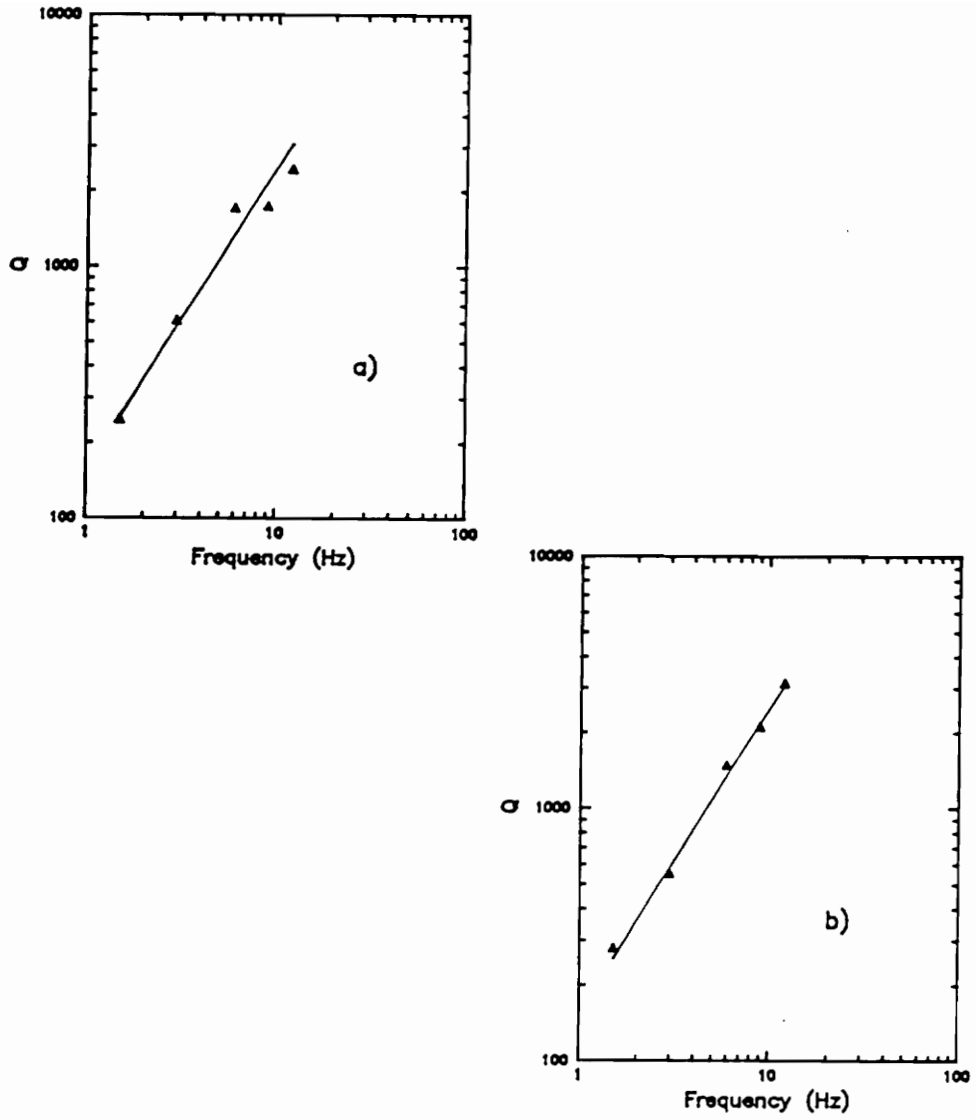

Figure 18. Q_{L_g} results from RTSM: Representative source-station grouping results from RTSM for western and central Virginia: a) eastern Kentucky blast and central Virginia blast and b) southwest Virginia earthquake and central Virginia blast.

Q_{Lg} was also estimated for Virginia and its environs using the Reversed Two Station Method (RTSM) of Chun and others (1987). Because of the symmetric source - station configuration necessary for this method only a limited number of Q_{Lg} estimates were possible. An unusually large quarry explosion in central Virginia was paired with a representative eastern Kentucky coal mine blast and a southwestern Virginia earthquake (see Table 2) to generate ten estimates of Q_{Lg}. Chun and others (1987) state that stable Q_{Lg} estimates may be made with only two or three source - station groupings. From the ten RTSM estimates of Q_{Lg} made using the two source - station groupings, the frequency dependence of Q_{Lg} in the crust of the Virginia area can be represented by $Q_o = 155$, $\sigma_{\log Q_o} = 0.1$, and $N = 1.2 \pm 0.2$. Q_{Lg} - f plots from two RTSM groupings are shown in Figure 18. These values are in agreement with those obtained using the Lg spectral method.

Q_C

The temporal decay of coda wave power spectra across the Giles County VTSO subnetwork was studied to estimate Q_C for the crust in western Virginia. This is basically an estimate of Q_C within the Giles County seismic zone. Q_C was found to be frequency dependent in the range 1 to 10 Hz: $Q_C(f) = Q_o f^N$. Coda waves from four local and near regional earthquakes (epicentral distances 6 - 260 km, magnitudes 2.1 - 3.2, depths 3 - 15 km) were used in this study. Lapse times (time after origin time) for the analysis ranged from 10 to 200 seconds. The results of the power spectra analysis can be represented by:

873311859	$Q_o = 293$	$\sigma_{\log Q_o} = 0.16$	$N = 0.9 \pm 0.2$
860851635	$Q_o = 74$	$\sigma_{\log Q_o} = 0.09$	$N = 1.5 \pm 0.9$
873250103	$Q_o = 260$	$\sigma_{\log Q_o} = 0.16$	$N = 0.8 \pm 0.2$
880471527	$Q_o = 118$	$\sigma_{\log Q_o} = 0.11$	$N = 1.3 \pm 0.1$
Combined data	$Q_o = 111$	$\sigma_{\log Q_o} = 0.07$	$N = 1.3 \pm 0.07$.

Figures 19 and 20 show plots of these results. The data points plotted are those with correlation coefficients from the $\log_{10}t_{?}^{?}P$ vs t plots greater than 0.5 (events 873250103 and 880471527 and combined data) and 0.7 (events 873311859 and 860851635).

The values obtained here are in agreement with the values determined studying the temporal decay of peak amplitudes from bandpassed seismograms. For four stations in the Giles County network recording one of the local earthquakes (860851635), the values of Q_C showed a frequency dependence that can be represented by $Q_o = 132$ and $N = 1.3$ (Figure 20).

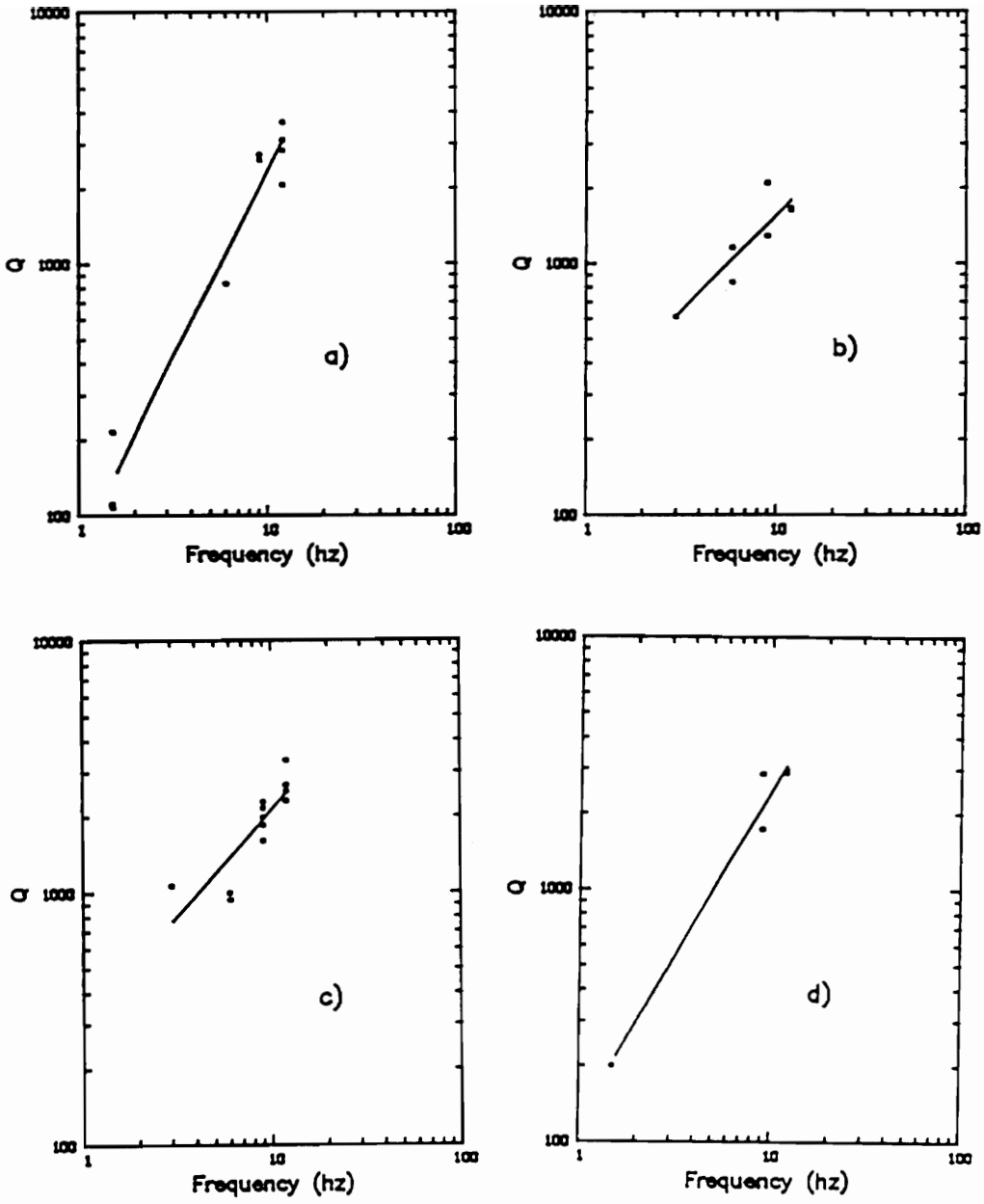

Figure 19. Q_c results for four earthquakes: Results from coda wave method for the four local earthquakes studied: a) 860851635 - Blacksburg, Virginia, b) 873250103 - Hillsville, Virginia, c) 873311859 - Lee County, Virginia, and d) 880471527 - Bristol, Virginia.

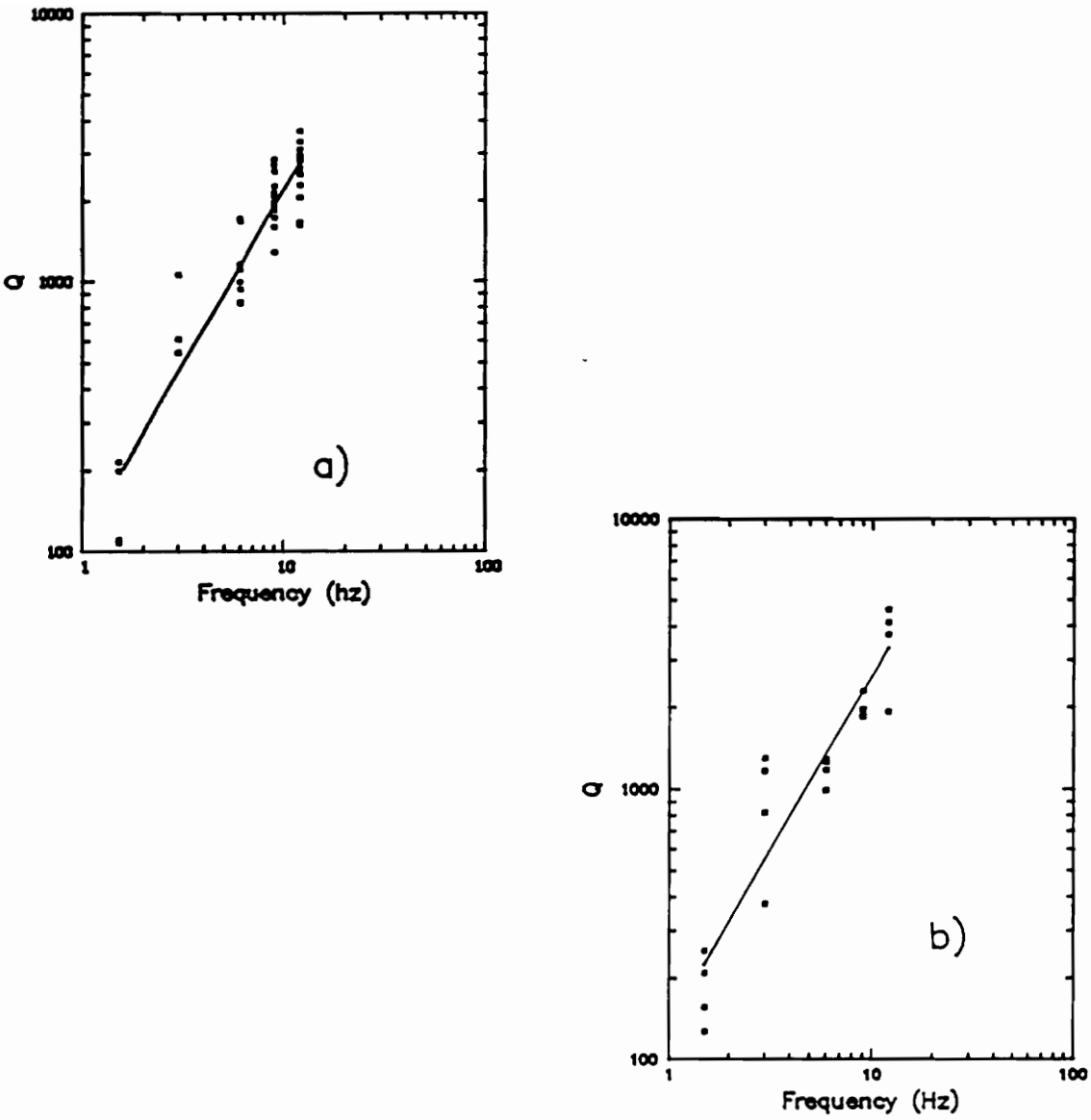

Figure 20. Q_c results from the two analysis methods: Q_c for western Virginia obtained using a) the frequency domain method, b) the time domain method.

Discussion

The Q_{Lg} and Q_C values reported herein are to be subjected to several comparisons; comparisons will be made between: **1)** results from the different methods to estimate Q_{Lg}, **2)** Q_{Lg} results obtained using earthquake data and explosion data, **3)** Q_C results from the frequency domain and time domain methods, and **4)** Q_{Lg} values and Q_C values. A comparison will then also be made between the results of this study and the results of previous published Q_{Lg} and Q_C studies for the eastern United States. The similarities and differences derived from these comparisons will be discussed and possible explanations offered.

Q_{Lg}

Q_{Lg} in the crust of Virginia and its environs as obtained by the Lg spectral method can be represented by $Q_{Lg}(f) = Q_o f^N$ where $Q_o = 186$, $\sigma_{\log Q_o} = 0.05$, and $N = 1.1 \pm 0.1$. This agrees with the power law relation obtained for the same region using the Reversed Two Station Method (RTSM) which showed $Q_o = 155$, $\sigma_{\log Q_o} = 0.1$, and $N = 1.2 \pm 0.2$. The similarity between these two results suggests that the effect of station site geology and topography is not as great as might be assumed. Or, if site effects and incorrect instrument corrections are present, problems related to them may

be removed by a qualitative editing process based on the comparison of signal spectra at all stations involved in the analysis, as was done in this study. This is an important conclusion for determination of attenuation trends in Virginia where the regional seismic activity occurs largely to the west of the seismic recording network. A situation such as that does not allow extensive use of the Reversed Two Station Method.

In a discussion of the merits of the RTSM versus non-reversed methods, Chun and others (1987) note that the presence of a site effect problem may cause errors as great as 300 percent in the determination of α ($\alpha = \pi f/QU$). In particular, they state that the determination of attenuation using two stations along the same azimuth from the source may cause problems *analogous to the complication in refraction seismology, which arises from the presence of dipping interfaces beneath the surface area*. That is, Lg attenuation may depend on Lg propagation direction. There was concern that such a directional dependence would cause anomalous Q_{L_g} results using the Lg spectral method in this study because the majority of sources were located to the west of the stations. The results of the RTSM, however, suggest that such a dependence does not exist for Q_{L_g} in the crust of the Virginia area or that it can be eliminated by using qualitative methods.

A comparison is also made between the Q_{L_g} results obtained using earthquake data, $Q_o = 149$, $\sigma_{\log Q_o} = 0.05$, and $N = 1.5 \pm 0.15$, and those from explosion data, $Q_o = 190$, $\sigma_{\log Q_o} = 0.06$, and $N = 1.1 \pm 0.15$ (see Figure 21). Considering the standard error, the values of Q_o for both data sets are comparable. The frequency dependence for the earthquake data, however, is approximately thirty percent higher than for the explosion data, although consideration of the standard errors involved brings them much closer together. It is concluded that the difference in the results of the two data sets is real. In addition to possible differences caused by a difference in source type, it is assumed that the Lg waves from the explosion and earthquake sources sample different regions of the crust. Campillo and others (1985) studied ray tracing of synthetic Lg waves with sources at various depths and showed that the Lg sampling region varies with source depth. The results here indicate that Q_{L_g} in the Virginia area exhibits a somewhat greater frequency dependence for the whole crust (results from earthquakes at depths 5 - 26 km) than for just the upper crust sampled by the surface explosion sources.

Q_c

The values of Q_C for the crust of western Virginia obtained using a frequency domain method ($Q_o = 111$, $N = 1.3$) and a time domain method ($Q_o = 132$, $N = 1.3$) are nearly identical (see Figure 21). This similarity suggests that the use of either type of method is equally valid for the determination of Q_C from local earthquake data. There is less scatter in the time domain data, but more subjectivity in the required fitting of decay envelops to bandpassed seismograms. The choice of a method should depend on the data base available and the problem being addressed.

Q_{L_g} compared with Q_c

Numerous comparisons have been made between the results of Q_{L_g} and Q_C analyses in a given region (Dwyer and others, 1984; Mitchell and Hwang, 1987; Rogers and others, 1987). The basis of these comparisons is the attempt to determine the nature of Lg waves and seismic coda waves and the degree to which Q_{L_g} and Q_C analyses are measuring the same attenuation processes.

Aki (1985) states that both observations and theoretical studies support the theory that coda waves are **backscattered S waves.** Q_C measurements, therefore, estimate the attenuation of S waves in the lithosphere as due to scattering by small scale heterogeneities **in addition to** intrinsic, anelastic absorption. Campillo and others (1985) model Lg waves as surface waves composed of multiple supercritically reflected S waves trapped in the crust or a crustal low velocity zone. The part scattering plays in Lg attenuation in their model is less clear. Mitchell and Hwang (1987) summarize the problem well by stating that the *latter part of the Lg phase is at least partly produced by scattering process* but that the *relative extent to which intrinsic attenuation and scattering each affect the early part of the Lg phase is as yet unknown.* They note that published Q_{L_g} and Q_C results are approximately the same for regions where they have both been estimated.

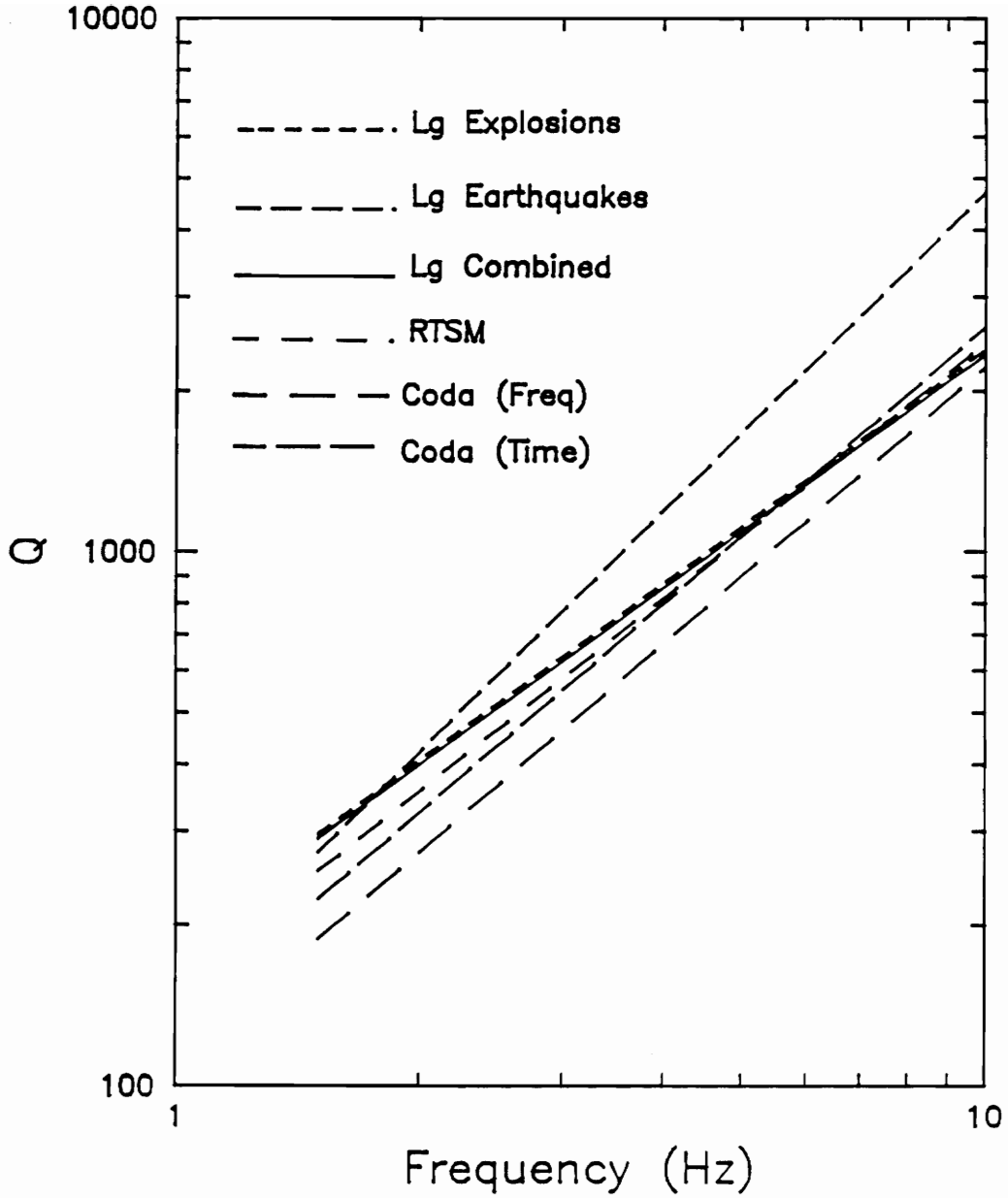

Figure 21. Q_{Lg} and Q_C results from the different analyses: Q_{Lg} results: explosion data, earthquake data, combined data, RTSM results; Q_C results: frequency domain method, time domain method.

The Q_{Lg} and Q_C results from this study are, indeed, very similar (see Figure 21). For the Lg spectral study, combined data can be represented by $Q_o = 186$, $\sigma_{\log Q_o} = 0.05$, and $N = 1.1 \pm 0.1$ and earthquake data can be represented by $Q_o = 149$, $\sigma_{\log Q_o} = 0.05$, and $N = 1.5 \pm 0.15$. The earthquake coda wave study results can be represented by $Q_o = 111$, $\sigma_{\log Q_o} = 0.07$, and $N = 1.3 \pm 0.07$. The similarity of the results for the two wave types indicates that similar attenuation mechanisms are operative in both Q_C and Q_{Lg} estimates. In particular, it appears that both energy loss by anelastic attenuation and energy redistribution by scattering are being measured by these values. Also, if both coda waves and the Lg phase are comprised of S waves, the attenuation of the two wave types should be similar. The similarity of the results lends support to the coda wave and Lg phase models used in this study.

Comparison of regional results

A comparison can also be made between the values of Q_{Lg} and Q_C obtained in this study and values of Q_{Lg} and Q_C reported for the eastern United States in previous published studies. As can be seen in Table 6, the values of Q_o and N obtained in this study for Virginia and its environs differ significantly from previous results reported for New England, the Appalachians, and the eastern United States in general. The previous Q_{Lg} regional results can be represented by an average $Q_o = 1003 \pm 289$ and average $N = 0.4 \pm 0.1$ whereas the combined Q_{Lg} results here can be represented by $Q_o = 186$, $\sigma_{\log Q_o} = 0.05$, and $N = 1.1 \pm 0.1$. The previous Q_C regional results can be represented by an average $Q_o = 500 \pm 332$ and average $N = 0.6 \pm 0.33$ whereas the combined Q_C results here can be represented by $Q_o = 111$, $\sigma_{\log Q_o} = 0.07$, and $N = 1.3 \pm 0.07$. Pulli (1984) reported Q_o and N values similar to those presented here for his study of New England for lapse times less than 100 seconds. Rhea (1984) obtained $Q_o = 190$, $N = 0.94$ for the South Carolina coastal plain.

Perhaps a more appropriate comparison of results, however, would be a comparison of results at 6 Hz. Modified Mercalli effects are believed to be caused by ground motion in this frequency

Table 6. Lg and coda Q results for the eastern United States.

Location	Q_{Lg} (1 Hz)	N	Source Type	Reference
Eastern U. S.	1000	0.35	Earthquakes	Goncz and Dean (1986)
Eastern U. S.	800	0.32	Earthquakes	Gupta and McLaughlin (1987)
Appalachians	1413	at 1 Hz	Earthquakes	Gupta and McLaughlin (1987)
Appalachians	1127	at 3 Hz	Earthquakes	Gupta and McLaughlin (1987)
Eastern U. S.	800	0.5	Earthquakes	Nuttli (1981)
Virginia	190	1.1	Explosions	This study
Virginia	149	1.5	Earthquakes	This study
Virginia	186	1.1	Combined	This study

Location	Q_c (1 Hz)	N	Source Type	Reference
S. Carolina	190	0.94	Earthquakes	Rhea (1984)
New England	140	0.95	Earthquakes	Pulli (1984) $t_t < 100$ sec
New England	660	0.4	Earthquakes	Pulli (1984) $t_t > 100$ sec
New England	460	0.40	Earthquakes	Pulli (1984) average t_t
Eastern U. S.	700-1000	0.3-0.4	Earthquakes	Singh (1981)
Virginia	293	0.9	Earthquake	This study
Virginia	260	0.8	Earthquake	This study
Virginia	74	1.5	Earthquake	This study
Virginia	118	1.3	Earthquake	This study
Virginia	111	1.3	Earthquakes	This study

Table 7. Values of Q_c for the United States standardized to 6 Hz.

Location	Study area (km^2)	Q_c(6 Hz)	Reference
South Carolina	35,000	1024	Rhea (1984)
New England	32,000	768	Pulli (1984)
New England	350,000	1351	Pulli (1984)
Eastern U. S.	5,500,000	1498	Singh (1981)
Western Virginia	3,000	1140	This study
Western Virginia	3,000	1356	This study
Basin and Range	600,000	560	Singh and Herrmann (1983)
Great Basin	90,000	644	Rogers and others (1987)
Western U. S.	2,700,000	735	Singh (1981)

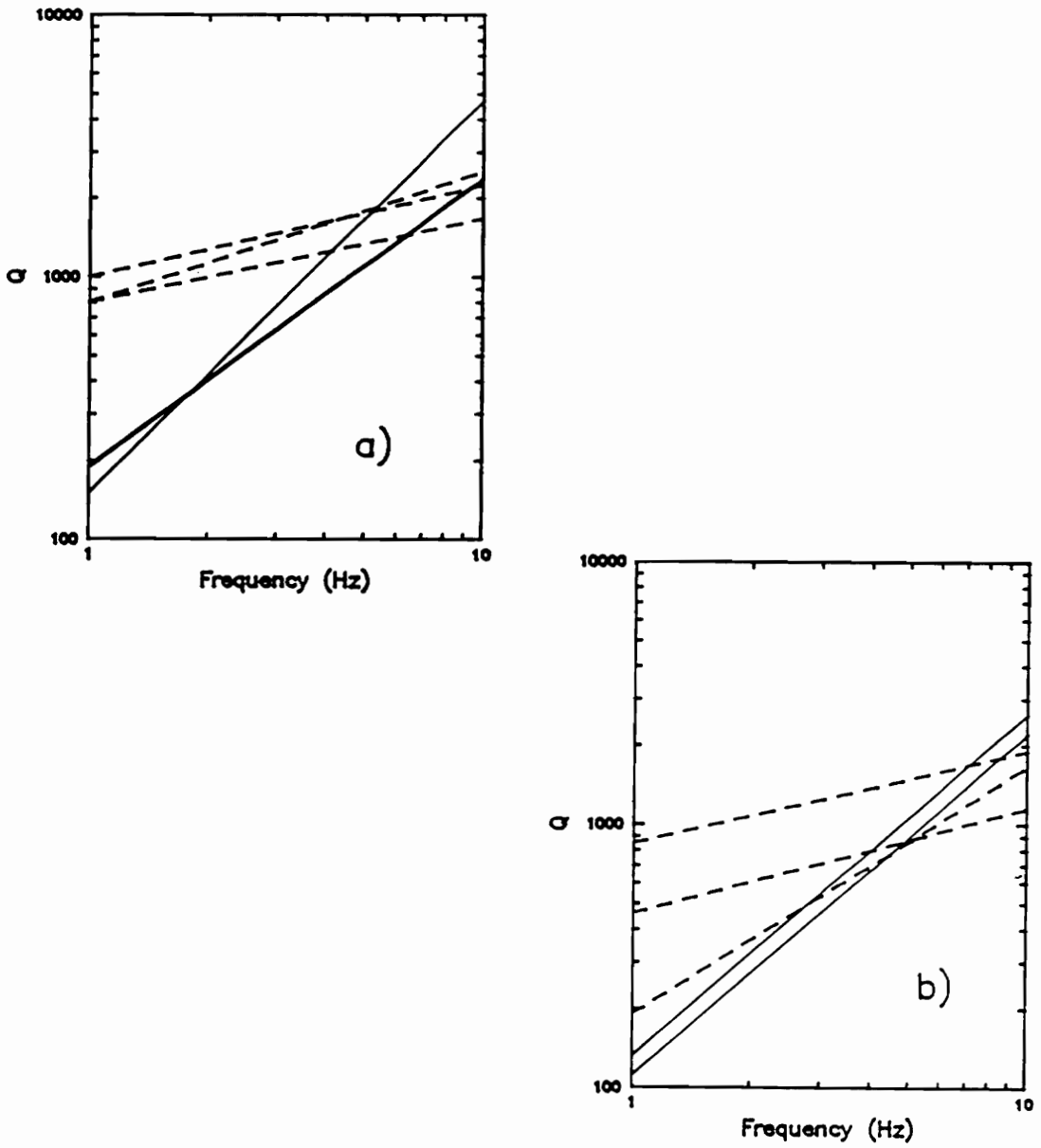

Figure 22. Q_{L_g} and Q_C for the eastern United States: Trends of observed quality factors for the eastern U. S. from the references cited in Table 7. a) Q_{L_g} results, b) Q_C results. Note that the plots of the results of this study (solid lines) cross those of previous studies (dashed lines) at approximately 6 Hz.

range. The results of several U. S. coda Q studies, as interpolated to 6 Hz, are shown in Table 7. Plots of Q_{Lg} and Q_C results for the eastern U. S. are combined in Figure 22. From Figure 22, it can be seen that the plots of Q_{Lg} and Q_C for this study cross those of previous eastern U. S. studies at approximately 6 Hz. Table 7 shows that the observed quality factors (anelastic attenuation and scattering) for the western and eastern U. S. (this study included) indicate a greater attenuation of seismic waves in the west than in the east. This is as expected from felt area and isoseismal decay with distance studies (Nuttli and Zollweg, 1974; Sibol and Bollinger, 1987).

Several possible explanations for these similarities and differences are presented in the following pages of this discussion.

Geometrical spreading models: The analysis performed in this study involves working with spectral amplitude or power data in the frequency domain. Many of the previous regional studies used analysis techniques in the time domain. The basic theory difference between working in the time domain and in the frequency domain involves the modeling of geometrical spreading. Time domain studies such as those performed in the eastern United States by Nuttli (1981), Goncz and Dean (1986), and Gupta and McLaughlin (1987) use a time domain geometrical spreading term of $R^{-0.833}$. The Lg spectral method used here models geometric spreading as $R^{-0.5}$ because the analysis is performed in the frequency domain (Nuttli, 1981; Hasegawa, 1985), see Appendix A.

Because of the significant difference between our Lg frequency domain results and previous time domain results, several Lg events were re-analyzed using a geometrical spreading term of $R^{-0.833}$. This changed equation (3) to $\log_{10}A(f,t,R) + 0.833\log_{10}R = \log_{10}S(f) - \frac{1.364ft}{Q_{Lg}(f)}$. The effect of changing the geometrical spreading coefficient to $R^{-0.833}$ was to increase the Q_o values by approximately 200 percent. The values of N changed by $\pm$ 1 percent, Figure 23. If Lg geometrical spreading should be corrected by $R^{-0.833}$ in the frequency domain, our Q_o values would be closer to those of previous studies than they are now. The change of the spreading exponent, however, does not effect the values of N enough to make them similar to previous results.

There are other examples where analyses done in the time domain and frequency domain in the same region produced significantly different results. Chávez and Priestley (1986) and Rogers

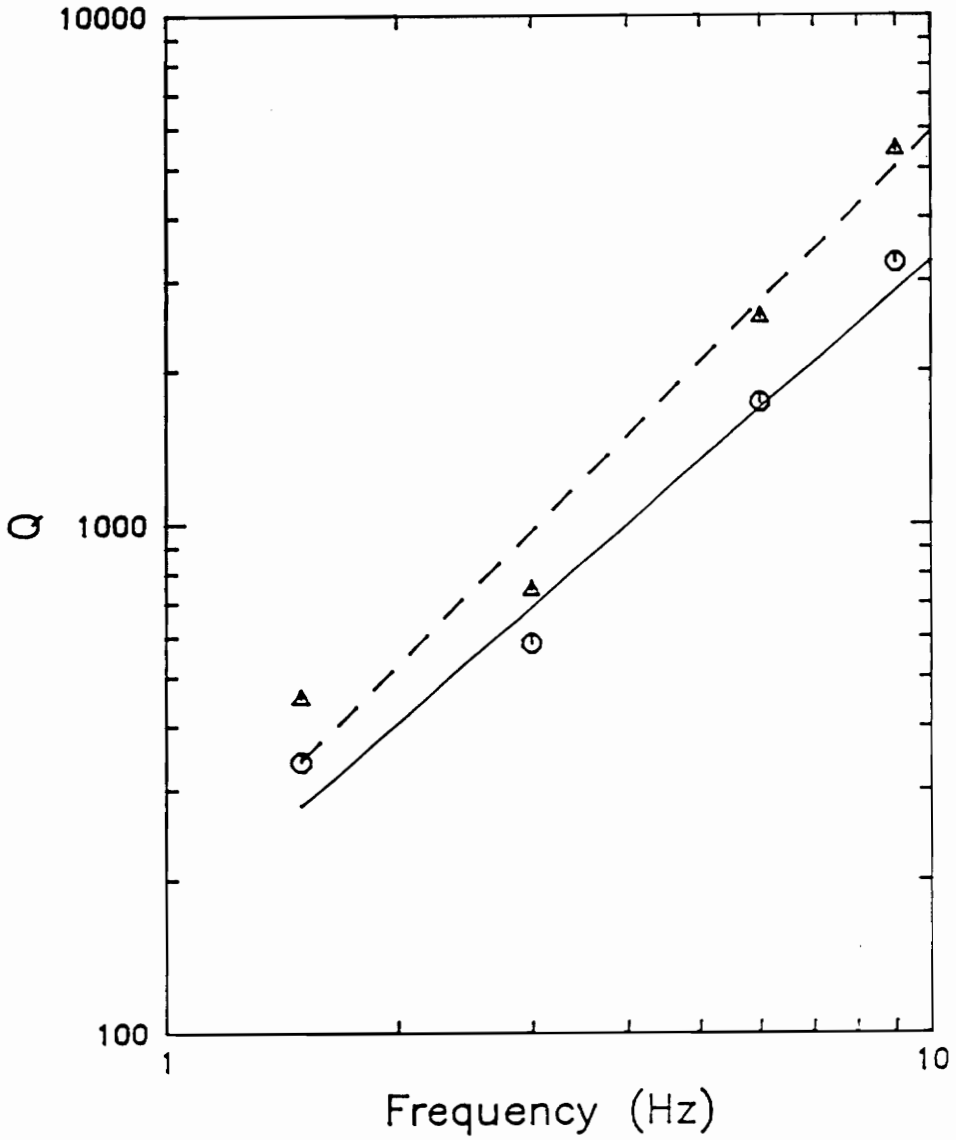

Figure 23. **The effect of changing geometrical spreading correction on Q_{L_g} results:** Q_{L_g} vs frequency plot for data analyzed using geometrical spreading coefficient of -0.5 (solid line, circles) and -0.833 (dashed line, triangles).

and others (1987) both report values of Q_{L_g} for the Great Basin of Nevada and California. Rogers and others' (1987) time domain regression technique yielded $Q_o = 774$ and $N = 0.04$ for the Great Basin at frequencies 3 - 10 Hz. Chávez and Priestley (1986) used the frequency domain Lg spectral method and obtained $Q_o = 214 \pm 15$ and $N = 0.54 \pm 0.09$ in the frequency band 0.3 - 5 Hz for earthquake data and $Q_o = 206$ and $N = 0.68$ in the frequency band 0.3 - 10 Hz for Nuclear Test Site explosion data.

The difference between the time domain method and the frequency domain method results in the Great Basin reported in these two studies is of the same nature as the difference between the frequency domain Q_{L_g} results of this paper and the time domain results of previous studies. The values of Q_o obtained using frequency domain techniques are lower than those obtained using time domain methods (206-214 versus 774, Great Basin; 149-190 versus 800-1400, eastern U. S.). The values of the frequency dependence, N, are greater for frequency domain methods than time domain methods (0.54-0.68 versus 0.04, Great Basin; 1.1-1.5 versus 0.3-0.5, eastern U. S.).

Some amount of model dependency may exist in the estimation of Q_{L_g} and Q_C frequency dependences. Others have cited the possibility of methodology related results (Chun and others, 1987; Gupta and McLaughlin, 1987), but the exact reasons for such method dependencies have not been determined. One possibility may be related to the effect of differing geometrical spreading coefficients on the results. Changing the geometrical spreading term used in the models tends to change values of Q_o. There is no apparent effect on the N values, however. While we do not believe that the use of $R^{-0.5}$ in the frequency domain and $R^{-0.833}$ in the time domain is incorrect, the effect these corrections have on the results has implications as to the models of coda waves and the Lg phase. If the coda is not made up solely of body waves and the Lg phase is not strictly a surface wave, different geometrical spreading coefficients than those now used would be required in the models. Pulli (1984) notes that for the development of coda waves, surface wave scattering may be a factor at low frequencies ($\simeq$1.5Hz) and short lapse times ($<$ 100 sec). Also, if Q_{L_g} measurements include the effects of scattering, there is a possibility that the Lg waves are converted to body waves as they encounter heterogeneities. Here, the model of Lg phase geometrical spreading as strictly surface

wave spreading is not correct. New models adjusted to account for varying geometrical spreading effects may result in Q_{L_g} and Q_C values that differ from any previous results.

Another possible explanation for the difference in results between time domain and frequency domain studies is mentioned by Chávez and Priestley (1986): *perhaps [such] discrepancies are indicative of the larger scatter inherent in time domain measurements of frequency dependent quantities.*

Site effects: One major concern during this study was the effect varying station site factors might have on our results. Two different techniques were used to attempt to remove site effects from our results.

The first was a qualitative removal of data that appeared inconsistent with the majority of the spectral data studied. A spectral comparison was made and stations that had shapes or amplitudes significantly different than the other stations recording the same event were considered contaminated by station site effects and/or incorrect station calibrations and were removed from analysis.

The second form of site effect related Q_{L_g} estimation used the RTSM. Although we had difficulty finding events that fell on a great circle path with two stations, we were able to obtain ten sets of Q_{L_g} estimates with the station site effects removed. The results of this analysis were consistent with the qualitative site effect removal results. As stated previously, these consistent results were considered support for using a qualitative site effect removal process if sources and stations are not in such locations as to warrant the use of the RTSM. The $Q_{L_g}(f)$ results of the two site effect removal processes can be represented by Q_o in the range 149-190 and $N \simeq 1.2$.

In addition to these two site effect correction techniques, station site responses were determined for the majority of the VTSO stations using a residual Q_{L_g} analysis technique. These station site responses may be used as site correction terms in future, more extensive Q_{L_g} studies.

Area of analysis: The general purpose of Q_{L_g} and Q_C studies is to gain some knowledge of the nature of regional seismic energy attenuation. While the estimation of Q_{L_g} and Q_C for large regions such as the eastern United States is important for hazard studies, the determination of regional

(study area of radius about 300 km) and local (study area of radius about 100 km) attenuation is of particular importance for the estimation of seismic hazard potential for specific areas.

In addition to the use of different geometrical spreading terms for time domain and frequency domain models, another difference between this study and other Q_{L_g} and Q_C studies in the eastern United States is the extent of the study areas. The regions for which Q_{L_g} and Q_C were estimated here are shown in Figures 2 - 5. Figure 5 shows the combined areal extent of all parts of this study. The region studied covers an area of approximately 400 × 800 km. As mentioned in the introduction, the study area is contained within the Piedmont, Blue Ridge, Valley and Ridge, and the eastern portion of the Appalachian plateau provinces. The average source - station distance for the Lg study is about 350 km. The coda Q study area is contained within the Lg study area and consists of a region of approximately 100 × 300 km (lapse times 10 - 200 seconds). This region is contained within the Valley and Ridge province, with one source located in the eastern Appalachian plateau province. The average source - station distance for the Q_C study is 100 km.

Previous coda wave and Lg attenuation studies in the eastern United States cover a much greater area than this study. Gupta and McLaughlin (1987) reported Q_{L_g} values for the eastern U. S. from the study of earthquakes that occurred and were recorded east of approximately 98°W, Figure 24. This is an area considerably larger than that considered here, Figure 5. Gupta and McLaughlin (1987) also report values of Q_{L_g} for the Appalachians. Their study includes the entire extent of the Appalachian mountains in the U. S. whereas this study focuses on a much smaller region crossing the border of the Plateau with the central and southern Appalachians. Nuttli (1981) studied Lg wave attenuation in the entire eastern U. S. (east of the Interior Highlands, ≃90°W).

Singh (1981) developed contour maps of Q_C for the continental United States. The study was then regionalized and values were reported for various regions. His estimates of Q_C for the eastern U. S. are for the area east of the Interior Highlands, using lapse times approximately 10 - 1000 seconds. Pulli (1984) studied Q_C in New England. Working with lapse times less than 100 seconds, he estimated Q_C for southern New Hampshire and eastern Massachusetts only (≃200 × 200 km) . The study area was extended to include all of New England (≃350,000 km²) by use of longer lapse

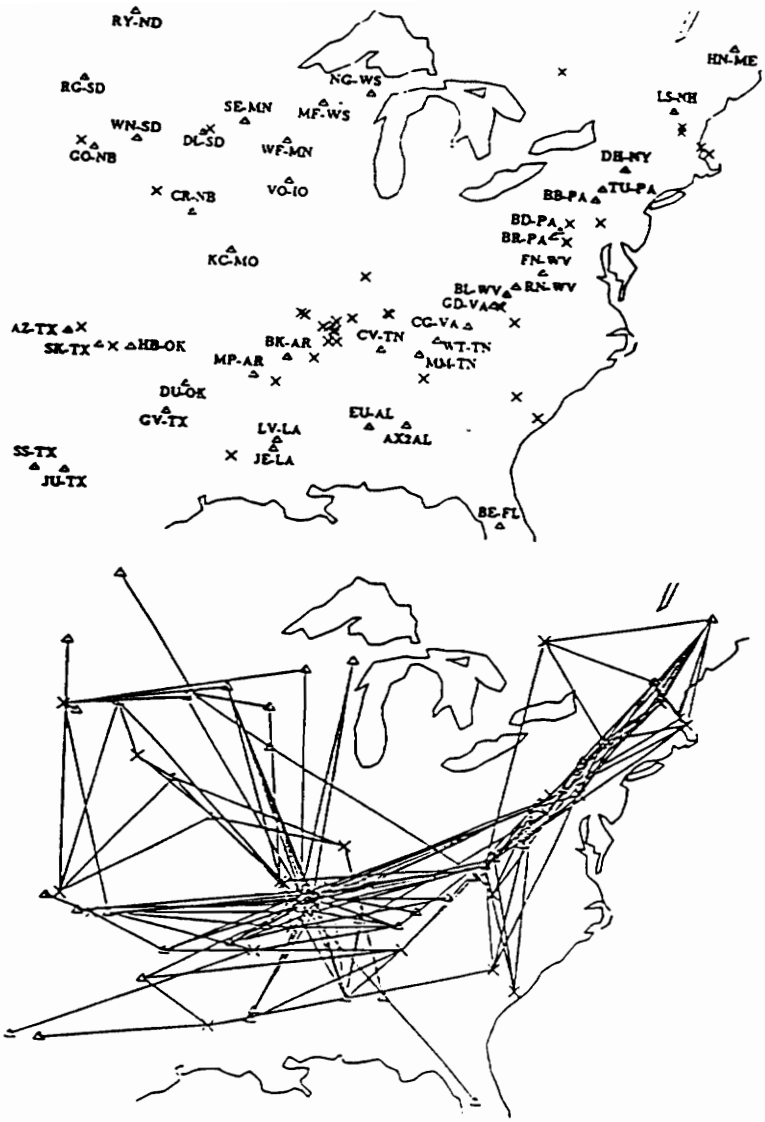

Figure 24. Study area from Gupta and McLaughlin (1987): Region of the United States designated as the eastern United States by Gupta and McLaughlin (1987). Shown here as a basis for Lg study area comparisons between this study and previous Lg Q studies in the eastern U. S.

times. Rhea (1984) estimated Q_C for an area of approximately 35,000 km² in the South Carolina coastal plain.

Gupta and McLaughlin (1987) make several points apropos of study area differences. They propose that differences between Q_o and N values for Q_{L_g} studies in the eastern U. S. are caused by lateral variations in crustal attenuation. Attenuation studies that make estimates of Q_{L_g} and Q_C for the entire eastern U. S. may be smoothing out regional and local variations of $Q_{(L_g,C)}(f)$ which differ significantly from the overall values. Pulli (1984) obtained estimates of Q_C at lapse times less than and greater than 100 seconds. The lower lapse times study resulted in values of Q_o less than, and N greater than, the values for longer lapse times. These results indicate that the smaller area (lower lapse times) had a different Q_C trend than the larger area studied. Gupta and McLaughlin (1987) note that there is evidence in their results of substantial regional variations in crustal attenuation at 1 Hz and possibly at 3 Hz. It is at these lower frequencies that the results of this study differ most significantly from the results of previous studies of the eastern U. S.

The assumption of the single scattering theory (Aki and Chouet, 1975; Sato, 1977) versus multiple scattering may play a part in the estimation of Q_C for various areas. Both Pulli (1984) and Rogers and others (1987) note that single scattering is an appropriate coda model for short lapse times, but multiple scattering is most likely involved in long lapse time coda formation. The effect of neglecting multiple scattering at long lapse times is an overestimation of Q_C. The high Q_o values obtained in Q_C studies of the eastern U. S. (as opposed to the Q_o values obtained for the Virginia area) may to some extent be overestimations caused by not modeling multiple scattering when such mechanisms do in fact exist.

Tectonic regimes: In addition to the analysis area differences between this study and other eastern U. S. studies, the volumes involved in the analyses are also different. The larger study areas for eastern U. S. attenuation estimates also correspond to larger study volumes in which the waves sample both the upper and lower crust and upper most mantle. A comparison of the results of this study and previous, more extensive studies indicates that the frequency dependence of Q_{L_g} and Q_C for the crust is greater than for the crust and mantle combined. This implies that the mantle is

more homogeneous than the crust. That is, scattering by heterogeneities is more prevalent in the crust than in the mantle and, hence, $Q_{(L_g,C)}$ values are lower for the crust.

The entire eastern United States (east of the Rocky Mountains) contains regions of varying seismicity and geologic structures. The area studied in this paper contains three well defined seismic zones within a folded and thrusted area of approximately 32,000 km^2 . Aki (1980) suggests that in tectonically active areas the lithosphere is highly heterogeneous, so the amount of seismic wave scattering is greater than in tectonically stable, homogeneous regions. The seismic zones included in this study area are active and so the low Q_o values and high N values estimated for the area are consistent with Aki's (1980) theory. The higher Q_o and lower N values obtained for the entire eastern U. S. may be the result of a bias from areas of lower seismic activity and more homogeneous crust within the eastern United States.

Conclusions

An additional aspect of our results needs to be considered. The frequency dependences of Q_{L_g} and Q_C observed here are of the form $Q_{(L_g,C)}(f) = Q_o f^N$. The values of N obtained using various methods range from 0.8 to 1.5. For frequency dependences of the form shown above, values of N greater than 1.0 imply that the seismic waves studied are being attenuated less at higher frequencies than at lower frequencies for the range 1 - 10 Hz. This seems to suggest that some unusual mode of propagation in which higher frequency waves propagate with low attenuation is present in the area. The data and processing used here are investigated in an attempt to determine what the high frequency dependence values represent.

In the Lg spectral analysis, the Lg amplitude spectra at all stations recording an event were compared. Figure 11 shows an example of spectra from different stations from the same explosion event. With increasing frequency, the spectra at different distances converge and, in some cases, cross each other. Data such as this would be represented by observed quality factors with frequency

dependence greater than one. This shows that the high frequency dependences are not introduced by our analysis technique.

Low signal-to-noise ratios are proposed as a possible explanation of our high frequency dependences. An analysis of the spectra shown in Figures 10 and 11 (the same event, a representative noise spectra is shown in Figure 10) indicates that, in this event, as with most others studied, the noise level is well below the level of the Lg amplitude spectra and is not considered a cause of the converging spectra.

Incorrect instrument corrections might cause amplitude spectra to converge and/or cross at higher frequencies. We admit that, on any given day, any given station might need calibration and, hence, the instrument correction performed for that station might be inaccurate. We believe, however, that over the extent of this study, the VTSO stations were well calibrated and the instrument corrections performed were correct. In addition to this, a qualitative removal of inconsistent looking station spectra was performed to remove data believed inaccurate due to station site responses and/or incorrect instrument correction. We have already determined that this method of data editing was successful and, hence, do not believe that incorrect instrument corrections are causing our high frequency dependence results.

We have also, using a limited number of observations, determined that site effect free estimates of Q_{L_g} in the Virginia area obtained using the RTSM are consistent with our other Lg results, so that local site effects are not causing our high N results. The application of the site correction terms, obtained using the Q_{L_g} residual method, to a larger data set in this same region should help in quantifying any effects of site response that were overlooked in this study. An analysis of the site correction terms indicates that local site effects have at most a factor of three effect on amplitude data in this area, and an effect as great as this is rare.

An investigation into our highly frequency dependent results for coda Q studies raises some questions about coda wave modeling. A few other coda Q studies have obtained frequency dependence values approaching or greater than one. Most notable are the results of Pulli (1984), Rhea (1984), and Rogers and others (1987). Pulli's (1984) results for southern New Hampshire and eastern Massachusetts showed a Q_C frequency dependence of $N = 0.95$. Rhea (1984) obtained N

values ranging from 0.79 to 1.16 for the South Carolina coastal plain. Rogers and others (1987) results for the southern Great Basin of Nevada and California showed a Q_C frequency dependence of 0.84 for earthquake data and 1.05 for nuclear explosion data. It is interesting to note that, as in this study of the Virginia area, these three studies showed highly frequency dependent results for small areas ($\simeq$32,000 – 90,000 km^2) within significantly larger regions for which much lower frequency dependences have been reported.

Pulli (1984) and Rogers and others (1987) cite that the modeling of coda waves as single backscattered waves may not be appropriate for all distances. Richards and Menke (1983) discuss the applicability of the coda power model (equation 5) to all study areas. They state *as long as the medium is anelastic and is in fact so weakly scattering that only primary reflections are important this [model] gives reliable estimates of Q. However, if the heterogeneity is sufficiently strong that multiple scattering is important and causes attenuation, these estimates of anelastic Q may be biased.*

The results of their modeling of multiple scattering may be used to interpret the high frequency dependence values obtained in this study. Highly frequency dependent coda Q values may be interpreted as being representative of a region where scattering dominates over anelastic attenuation. Richards and Menke (1983) state that dominant scattering in a region is represented by coda Q approximately proportional to frequency and observed Q values determined from direct waves that are frequency independent.

If we can assume that Lg waves are not direct waves and are affected to some extent by scattering, the high Q_{L_g} frequency dependence obtained here may again be considered an indication that scattering predominates over anelastic attenuation in the Virginia area.

The scatter in our high frequency data may be indicative of this phenomena. Higher frequency data contains information from more wavelengths for a given distance than lower frequency data, and hence, better definition is expected. In the situation here, however, the higher frequency data are probably being contaminated by scattering effects, decreasing the amount of definition in the data for a given distance. So, the large frequency dependence values for our observed quality factors Q_{L_g} and Q_C ($N\simeq1.1$) do not represent a mode of propagation in which higher frequency waves are attenuated less than lower frequency waves. Remember that Q_{L_g} and Q_C do not represent just

anelastic attenuation, but rather more complex attenuation mechanisms including scattering effects. Our large frequency dependence results represent an area where scattering mechanisms dominate over anelastic attenuation as an amplitude decay mechanism.

It seems that a major problem in attenuation studies such as this one is that the decay models used may be too simplistic. Important problems that need to be addressed in future studies are:

- To what extent do observed quality factors measure anelastic attenuation?
- To what extent do they measure scattering?
- How much of an effect do site effects have on Q_{Lg} and Q_C results?
- Can site effect problems be completely removed from analysis?
- Are the models of coda waves as singly backscattered S waves and the Lg phase as a surface wave correct for all frequencies and all distances?
- If not, should geometrical spreading and scattering be modeled differently?

Until these questions are answered more clearly than they have been at this time and more complex models of attenuation are developed, comparisons of observed quality factors from different studies should not be performed without consideration of the models used and the extent of the areas studied.

Summary

The apparent quality factors Q_{Lg} (attenuation determined from the spatial decay of Lg waves) and Q_C (attenuation determined from the temporal decay of seismic coda waves) were estimated for the crust of Virginia and its environs. These two factors were determined to be frequency dependent; the results are presented in the form $Q_{(Lg,C)} = Q_o f^N$ where $Q_{(Lg,C)} = Q$ (1 Hz) and N represents the frequency dependence. The area studied is located in the Appalachian region of Virginia and eastern Tennessee and contains three zones of regionally high seismicity: the eastern Tennessee seismic zone, the Giles County seismic zone, and the central Virginia seismic zone. Estimates of Q_{Lg} were obtained using two different methods and the results for the frequency band 1 - 4 Hz are presented in Figure 21 and can be represented by:

Explosion data	$Q_o = 190$	$\sigma_{\log Q_o} = 0.06$	$N = 1.1 \pm 0.15$
Earthquake data	$Q_o = 149$	$\sigma_{\log Q_o} = 0.05$	$N = 1.5 \pm 0.15$
Combined data	$Q_o = 186$	$\sigma_{\log Q_o} = 0.05$	$N = 1.1 \pm 0.1$
RTSM	$Q_o = 155$	$\sigma_{\log Q_o} = 0.1$	$N = 1.2 \pm 0.2$.

Estimates of Q_C were obtained for the crust of western Virginia (the Giles County seismic zone) using a frequency domain method and the results for 1 - 10 Hz are shown in Figure 21 and can be represented by:

Combined data	$Q_o = 111$	$\sigma_{\log Q_o} = 0.07$	$N = 1.3 \pm 0.07$.

These Q_C results are in agreement with those obtained using a time domain method that showed $Q_o = 132$ and $N = 1.3$. This suggests that the use of either time domain or frequency domain techniques to estimate Q_C is valid.

The estimates of Q_C and Q_{L_g} are very similar, suggesting that the waves are sampling similar volumes and that the same attenuation mechanisms are measured in both cases. In particular, **both anelastic attenuation and scattering mechanisms must be measured by these factors.**

These results are different than previous Q_{L_g} and Q_C results reported for the eastern United States which generally show $Q_o \simeq 1000$ and $N \leq 0.5$. Several possible explanations are given for these differences. These can be summarized as follows:

- estimates of Q_{L_g} and Q_C may be affected by incorrect geometrical spreading models
- the size of the study area may affect Q_{L_g} and Q_C estimates
  - lateral variations in Q_{L_g} across geological provinces may be substantial at low frequencies (1 - 3 Hz)
  - the single scattering assumption may not be correct for Q_C at greater distances
- tectonically active zones have lower Q_o and higher N values than tectonically stable regions; the $Q_{(L_g,C)}$ estimates made for the entire eastern United States may be biased by tectonically stable areas.

In general, the changing of geometrical spreading models and scattering models both have only a factor of one to two effect on observed quality factor estimates (Gao and others, 1983; Pulli, 1984). The effect of the other factors mentioned above cannot be quantified.

The Q_{L_g} and Q_C results of this study are highly frequency dependent. This appears to suggest that a propagation mode exists in the region that allows higher frequency ($\simeq$10 Hz) waves to propagate more efficiently than lower frequency (1 Hz) waves. What must be remembered, however, is that these factors measure both anelastic attenuation and scattering effects. It is believed that the high frequency dependence values are indicative of an area where scattering for those wavelengths is dominant over anelastic attenuation.

These high frequency dependence results for the small ($\simeq$32,000 km^2) region of Virginia and its environs studied may help to explain the relatively small meizoseismal areas observed in the

southeastern United States (Evernden, 1975). If seismic energy is rapidly attenuated over small regions of the southeastern U. S., maximum intensity effects would be felt over only 'small' regions with respect to the total affected area. The low Q_o, high N values obtained by Rhea (1984) for the Charleston, South Carolina area ($\simeq$35, 000 km^2) also support this hypothesis.

The high frequency dependence results are extremely relevant. If the values of Q_{L_g} and Q_C obtained for the Virginia area are not biased by local site effects or varying source effects and if the results can be scaled with magnitude for the region *there should be increased concern about the effects of high frequency (6 - 10 Hz) waves on engineering structures in Virginia and its environs.*

References

Aki, K. (1969). Analysis of seismic coda of local earthquakes as scattered waves. *J. Geophys. Res.*, Vol. 74, pp. 615-631.

Aki, K. (1980). Scattering and attenuation of shear waves in the lithosphere. *J. Geophys. Res.*, Vol. 85, pp. 6496-6504.

Aki, K. (1985). Theory of earthquake prediction with special reference to monitoring of the quality factor of lithosphere by the coda method. *Earthquake Predict. Res.*, Vol. 3, pp. 219-230.

Aki, K. and B. Chouet (1975). Origin of coda waves: Source, attenuation, and scattering effects. *J. Geophys. Res.*, Vol. 80, No. 23, pp. 3322-3342.

Bollinger, G. A. (1973). Seismicity of the southeastern United States. *Bull. Seis. Soc. Amer.*, Vol. 63, pp. 1785- 1808.

Bollinger, G. A. and D. W. Griffiths (1979). The effect of Appalachian mountain topography on seismic waves. *Bull. Seis. Soc. Amer.*, Vol. 69, No. 4, pp. 1081-1105.

Bollinger, G. A., M. C. Chapman, and T. P. Moore (1980). *Central Virginia regional seismic network: Crustal velocity structure in central and southwestern Virginia.* NUREG/CR-1217, U. S. Nuclear Reg. Comm., Washington, DC, 187 pp.

Bollinger, G. A., J. A. Snoke, M. S. Sibol, and M. C. Chapman (1986). *Virginia Regional Seismic Network: Final Report (1977-1985).* NUREG/CR-4502, U. S. Nuclear Reg. Comm., Washington, DC, 57 pp.

Campillo, M., J. Plantet, and M. Bouchon (1985). Frequency-dependent attenuation in the crust beneath Central France from Lg waves: Data analysis and numerical modeling. *Bull. Seis. Soc. Amer.*, Vol. 75, No. 5, pp. 1395-1411.

Chávez, D. E. and K. F. Priestley (1986). Measurement of frequency dependent Lg attenuation in the Great Basin. *Geophys. Res. Letters*, Vol. 13, No. 6, pp. 551-554.

Chun, K., G. F. West, R. J. Kokoski, and C. Samson (1987). A novel technique for measuring Lg attenuation - Results from Eastern Canada between 1 to 10 Hz. *Bull. Seis. Soc. Amer.* Vol. 77, No. 2, pp. 398-419.

Dainty, A. M. and M. N. Toksöz (1981). Seismic codas on the Earth and the Moon: A comparison. *Phys. Earth Planet. Interiors*, Vol. 26, pp. 250-260.

Del Pezzo, E., F. Ferulano, A. Giarruso, and M. Martini (1983). Seismic coda Q and scaling law of the source spectrum at the Aeolian Islands, Southern Italy. *Bull. Seis. Soc. Amer.*, Vol. 73, No. 1, pp. 97-108.

Dwyer, J. J., R. B. Herrmann, and O. W. Nuttli (1983). Spatial attenuation of the Lg wave in the Central United States. *Bull. Seis. Soc. Amer.*, Vol. 73, No. 3, pp. 781-796.

Dwyer, J. J., R. B. Herrmann, and O. W. Nuttli (1984). Use of a digital seismic network to study regional Lg attenuation and coda Q in the Central Mississippi Valley (abstr). *Earthquake Notes*, Vol. 55, pp. 7-8.

Dysart, P. S., J. A. Snoke, and I. S. Sacks (1988). Source parameters and scaling relations for small earthquakes in the Matsushiro region, southwest Honshu, Japan. *Bull. Seis. Soc. Amer.*, Vol. 78, pp. 571-590.

Evernden, J. F. (1975). Seismic intensities, "size" of earthquakes and related parameters. *Bull. Seis. Soc. Amer.*, Vol. 65, No. 5, pp. 1287-1313.

Fehler, M., P. Roberts, and T. Fairbanks (1988). A temporal change in coda wave attenuation observed during an eruption of Mount St. Helens. *J. Geophys. Res.*, Vol. 93, No. B5, pp. 4367-4373.

Gao, L. S., L. C. Lee, N. W. Biswas, and K. Aki (1983). Comparison of the effects between single and multiple scattering on coda waves for local earthquakes. *Bull. Seis. Soc. Amer.*, Vol. 73, pp. 377-389.

Glover, L., III, J. A. Speer, G. S. Russell, and S. S. Farrar (1983). Ages of regional metamorphism and ductile deformation in the central and southern Appalachians. *Lithos*, Vol. 16, pp. 223-245.

Gonzc, J. H. and W. C. Dean (1986). Source spectral functions and path attenuation for Eastern United States regional phases by regression analysis of RSTN data (abstr). *Eos, Trans. Amer. Geophys. Union*, Vol. 67, p. 316.

Gupta, I. N. and K. L. McLaughlin (1987). Attenuation of ground motion in the Eastern United States. *Bull. Seis. Soc. Amer.*, Vol. 77, No. 2, pp. 366-383.

Harris, L. D. (1976).Thin-skinned tectonics and potential hydrocarbon traps - illustrated by a seismic profile in the Valley and Ridge province of Tennessee. *Jour. Res. U. S. Geol. Sur.*, Vol. 4, pp. 379-386.

Hasegawa, H. S. (1985). Attenuation of Lg waves in the Canadian Shield. *Bull. Seis. Soc. Amer.*, Vol. 75, No. 6, pp. 1569-1582.

Hatcher, R. D., Jr., J. R. Butler, P. D. Fullagar, D. T. Secor, and A. W. Snoke (1980). Geologic synthesis of the Tennessee - Carolinas - northeast Georgia southern Appalachians, in D. R. Wones (ed) *Proceedings: The Caledonides in the U. S. A.*, VPI and SU, pp. 83-90.

Herraiz, M. and A. F. Espinosa (1986). Scattering and attenuation of high-frequency seismic waves: Development of the theory of coda waves. *USGS Open-File Report 86-455*, 92 p.

Huang, Z. and M. Wyss (1986). S-coda before the 1983 Hawaii earthquake (abstr). *Eos, Trans. Amer. Geop. Union*, Vol. 67, No. 16, p. 315.

Jackson, D. D. and D. L. Anderson (1970). Physical mechanisms of seismic-wave attenuation. *Rev. Geophys. Space Phys.*, Vol. 8, pp. 1-63.

Johnston, D. H., M. N. Toksöz, and A. Timur (1979). Attenuation of seismic waves in dry and saturated rocks: II. Mechanisms. *Geophysics*, Vol. 44, No. 4, pp. 691-711.

Kanamori, H. and D. L. Anderson (1977). Importance of physical dispersion in surface wave and free oscillation problems: review. *Rev. Geophys. Space Phys.*, Vol. 15, No. 1, pp. 105-112.

King, J. L. and B. E. Tucker (1984). Observed variations of earthquake motion across a sediment-filled valley. *Bull. Seis. Soc. Amer.*, Vol. 74, No. 1, pp. 137-151.

Knopoff, L. (1964). Q. *Rev. Geophys.*, Vol. 4, No. 2, pp. 625-660.

Lahr, J. C. (1980). HYPOELLIPSE/MULTICS: A computer program for determining local earthquakes hypocentral parameters, magnitude and first motion pattern. *USGS Open-File Report 80-59*, 59 pp.

Liu, H., D. L. Anderson, and H. Kanamori (1976). Velocity dispersion due to anelasticity; implications for seismology and mantle composition. *Geophys. J. R. astr. Soc.*Vol. 47, No. 1, pp. 41-58.

Mitchell, B. J. and H. J. Hwang (1987). Effect of low Q sediments and crustal Q on Lg attenuation in the United States. *Bull. Seis. Soc. Amer.*, Vol. 77, No. 4, pp. 1197-1210.

Nowroozi, A. A. (1968). Measurement of Q values from the free oscillations of the earth. *J. Geophys. Res.*, Vol. 73, pp. 1407-1415.

Nuttli, O. W. (1978). A time-domain study of the attenuation of 10 Hz waves in the New Madrid seismic zone. *Bull. Seis. Soc. Amer.*, Vol. 68, No. 2, pp. 343-355.

Nuttli, O. W. (1981). Similarities and differences between western and eastern United States earthquakes, and their consequences for earthquake engineering, in J. E. Beavers (ed) *Earthquakes and Earthquake Engineering: The Eastern United States*, pp. 25-51.

Nuttli, O. W. (1986). Yield estimates of Nevada Test Site explosions obtained from seismic Lg waves. *J. Geophys. Res.*, Vol. 91, pp. 2137-2151.

Nuttli, O. W. and J. E. Zollweg (1974). The relation between felt area and magnitude for central United States earthquakes. *Bull. Seis. Soc. Amer.*, Vol. 64, pp. 73-85.

Peseckis, L. L. and P. W. Pomeroy (1984). Determination of Q using Lg waves and its implications for nuclear yield estimation. *Eos, Trans. Amer. Geophys. Union*, Vol. 65, p. 995.

Phillips, W. S. and K. Aki (1986). Site amplification of coda waves from local earthquakes in central California. *Bull. Seis. Soc. Amer.*, Vol. 76, pp. 627-648.

Pratt, T. L., C. Çoruh, and J. K. Costain (1987). Lower crustal reflections in central Virginia, USA. *Geophys. J. R. astr. Soc.*, Vol. 89, pp. 163-170.

Press, F. and M. Ewing (1952). Two slow surface waves across North America. *Bull. Seis. Soc. Amer.*, Vol. 42, pp. 219-228.

Pulli, J. J. (1984). Attenuation of coda waves in New England. *Bull. Seis. Soc. Amer.*, Vol. 74, No. 4, pp. 1149-1166.

Rautian, T. G. and V. I. Khalturin (1978). The use of the coda for determination of the earthquake source spectrum. *Bull. Seis. Soc. Amer.*, Vol. 68, No. 4, pp. 923-948.

Rebollar, C. J., C. Traslosheros, and R. Alvarez (1985). Estimates of seismic wave attenuation in Northern Baja California. *Bull. Seis. Soc. Amer.*, Vol. 75, No. 5, pp. 1371-1382.

Rhea, S. (1984). Q determined from local earthquakes in the South Carolina coastal plain. *Bull. Seis. Soc. Amer.*, Vol. 74, No. 6, pp. 2257-2268.

Richards, P. G. and W. Menke (1983). The apparent attenaution of a scattering medium. *Bull. Seis. Soc. Amer.*, Vol. 73, No. 4, pp. 1005-1021.

Rodriguez, M., J. Havsko, and S. K. Singh (1983). Q from coda waves near Petatlán, Guerrero, Mexico. *Bull. Seis. Soc. Amer.*, Vol. 73, No. 1, pp. 321-326.

Rogers, A. M., S. C. Harmsen, R. B. Herrmann, and M. E. Meremonte (1987). A study of ground motion attenuation in the southern Great Basin, Nevada - California, using several techniques for estimates of Q_s, $\log A_0$, and coda Q. *J. Geophys. Res.*, Vol. 92, No. B5, pp 3527-3540.

Sacks, I. S. and J. A. Snoke (1984). Structure and evolution of the continental lithosphere. *Phys. and Chem. of the Earth*, Vol. 15, pp. 3-37.

Sato, H. (1977). Energy propagation including scattering effects- single isotropic scattering approximation. *J. Phys. Earth,* Vol. 25, pp. 27-41.

Sato, H. and M. H. Manghanani (1985). Ultrasonic measurements of V_P and Q_P: Relaxation spectrum of complex modulus on basalt melts. *Phys. Earth Planet. Interiors*, Vol. 41, pp. 18-33.

Sibol, M. S. and G. A. Bollinger (1987). Quantifications of differences in the attenuation of Modified Mercalli Intensity between eastern and western North America. *Seism. Res. Ltrs.,* Vol. 58, p. 104.

Singh, S. (1981). *Regionalization of crustal Q in the continental United States.* [PhD dissertation] Saint Louis University, 184 pp.

Singh, S. and R. B. Herrmann (1983). Regionalization of crustal coda Q in the continental United States. *J. Geophys. Res.*, Vol. 88, pp. 527-538.

Stacey, F. D., M. T. Gladwin, B. McKavanagh, A. T. Linde, and L. M. Hastie (1975). Anelastic damping of acoustic and seismic pulses. *Geophysical Surveys*, Vol. 2, pp. 133-151.

Teague, A. G. (1984). *Focal mechanisms for Eastern Tennessee earthquakes, 1981-1983.* [MS Thesis] VPI & SU, 161 pp.

Teng, T-L. (1968). Attenuation of body waves and the Q structure of the mantle. *J. Geophys. Res.*, Vol 73, pp. 2195-2208.

Toksöz, M. N., D. H. Johnston, and A. Timur (1979). Attenuation of seismic waves in dry and saturated rocks: I. Laboratory measurements. *Geophysics,* Vol. 44, No. 4, pp. 681-690.

Tsujiura, M. (1978). Spectral analysis of the coda waves from local earthquakes. *Bull. Earthquake Res. Institute*, Vol. 53, pp. 1-48.

Tucker, B. E., J. L. King, D. Hatzfeld, and I. L. Nersesov (1984). Observations of hard-rock site effects. *Bull. Seis. Soc. Amer.*, Vol. 74, No. 1, pp. 121-136.

Waters, K. H. (1981). *Reflection seismology, 2nd edition*, John Wiley and Sons, New York, 453 pp.

Wehr, F. and L. Glover, III (1985). Stratigraphy and tectonics of the Virginia - North Carolina Blue Ridge: Evolution of a late Proterozoic - early Paleozoic hinge zone. *Geol. Soc. Amer. Bull.*, Vol. 96, pp. 285-295.

Appendix A. Derivation of spectral models

Intrinsic absorption model

When considering seismic attenuation two aspects are usually considered: the temporal decay of the amplitude of a standing wave at a fixed wave number and the spatial decay of a propagating wave at a fixed frequency. The relationship of these decay modes to the quality factor can be derived from the differential form of equation (1), $Q^{-1} = -(\Delta E)/(2\pi E)$. The general form of the following derivation is from Aki and Richards (1980, Chap. 5) and Stacey and others (1975).

Assuming a linear response of the material considered (i.e. elastic deformation proportional to stress), wave energy is proportional to the wave amplitude squared,

$$E \propto A^2. \qquad [13]$$

Differentiating this,

$$\Delta E \propto 2A\Delta A. \qquad [14]$$

Dividing (14) by (13), constants of proportionality cancel out and the result may be combined with (1) to yield

$$\frac{\Delta E}{E} = \frac{2A\Delta A}{A^2} = -\frac{2\pi}{Q}$$

or, after rearranging

$$\frac{1}{Q} = -\frac{\Delta A}{\pi A}. \qquad [15]$$

If we consider attenuation as the spatial decay of a propagating wave at a fixed frequency, then ΔA is the change in wave amplitude (dA) per distance traveled (dr) at a certain wavelength (λ),

$$\Delta A = \frac{dA}{dr}\lambda,$$

where the wavelength $\lambda = \frac{c}{f} = \frac{2\pi c}{\omega}$, c is the phase velocity, and f is the frequency. Substitutions into (15) yield

$$\frac{1}{Q} = -\frac{1}{\pi}\frac{1}{A}\frac{dA}{dr}\frac{2\pi}{\omega}c.$$

Rearranging and integrating both sides results in

$$\ln A = -\frac{\omega}{2cQ}r + \ln A_o$$

or

$$\ln\frac{A}{A_o} = -\frac{\omega}{2cQ}r$$

where $\ln A_o$ is a constant of integration. Taking the exponential of both sides and rearranging,

$$A(r) = A_o e^{-\omega r/2cQ}. \qquad [16]$$

This represents the spatial decay of amplitude in the direction of wave propagation and may be written as $A(r) = A_o e^{-\alpha r}$ where $\alpha = \frac{\omega}{2cQ}$ is the spatial attenuation coefficient.

The temporal decay of the amplitude of a standing wave at a fixed wave number may be obtained in a similar fashion. More simply, substitution of $r = ct$ into (16) yields

$$A(t) = A_o e^{-\omega t/2Q}. \qquad [17]$$

This may be written in terms of the time attenuation coefficient γ: $A(t) = A_o e^{-\gamma t}$ where $\gamma = \frac{\omega}{2Q}$.

Geometrical spreading model

As noted in the body of the text, however, the decay of seismic amplitudes as a wave propagates is not solely due to the intrinsic absorption represented by Q. As energy is spread out over increasingly larger wave fronts, the amplitude along a given ray path decreases. Geometrical spreading terms are included in amplitude decay models, such as those given in the main text, to account for this additional decay mechanism. Discussions of geometrical spreading models are given in Ewing and others (1957, pp. 143-144), Aki and Richards (1980, p. 212), Ben-Menahem and Singh (1981, pp. 266-269), and Bullen and Bolt (1985, pp. 185-186).

In general, for a flat earth model, geometrical spreading is modeled as $r^{-\nu}$ where r is epicentral distance and ν is the spreading coefficient which varies with wave type. Including such a term in equation (16) yields the amplitude decay equation

$$A(r) = A_o r^{-\nu} e^{-\omega r/2cQ} \qquad [18]$$

For body waves, $\nu = 1$; for head waves, $\nu = 2$; and for surface waves, $\nu = 1/2$. When dealing with surface waves, however, dispersion resulting from the velocity structure must be considered. Ewing and others (1957, pp. 143-144) noted that for "normal" modes, an additional fall-off term of $r^{-1/2}$ is necessary to account for dispersion and for Airy phases an additional fall-off term of $r^{-1/3}$ is necessary. So, for "normal" mode surface waves

$$A(r) = A_o r^{-1} e^{-\omega r/2cQ}$$

and for an Airy phase

$$A(r) = A_o r^{-5/6} e^{-\omega r/2cQ}.$$

In frequency domain computations, however, the attenuation of ground motion of higher-mode surface waves (Airy phase) is given by

$$A(r) = A_o r^{-1/2} e^{-\omega r/2cQ}.$$

In the frequency domain, one deals with discrete frequencies and dispersion is not a factor (Hasegawa, 1985; Nuttli, pers. comm.). This frequency domain model is of interest in the Lg spectral method used in this study.

Scattering model

In addition to intrinsic absorption and geometrical spreading, amplitude loss due to the redistribution of energy by scattering must be considered. To begin, let us introduce a source term $S'(\omega)$ that includes only source parameters, whereas the spreading and anelastic attenuation terms are part of a path term. The amplitude decay a temporal decay model becomes

$$A(t,\omega) = S'(\omega) t^{-\nu} e^{-\omega t/2Q}.$$

Aki (1969) considered the coda of local earthquakes to be comprised of scattered waves. We will cite his basic model as an example of the introduction of scattering losses to the amplitude decay model. First, we need to introduce the power spectra of a seismic event $P(\omega,t)$ which equals the square of the amplitude spectra:

$$P(\omega,t) = A^2(\omega, t) = S(\omega)\, t^{-\mu} e^{-\omega t/Q} \qquad [19]$$

where $S(\omega) = (S'(\omega))^2$ and $\mu = 2\nu$. The model proposed by Aki (1969) was for backscattered waves generated within an unbounded, homogeneous, and isotropic medium within which heterogeneities are randomly and two-dimensionally distributed on the surface. The heterogeneities are the scatterers which are considered to be greater in size than the wavelengths considered. No velocity perturbations or multiple scattering was allowed. The station and source are located at the same point.

This single backscattering model was used in this study as the model for the coda wave analysis. It is used to model the coda as the superposition of discrete scattering sources. Under these conditions, equation (19) becomes

$$P(\omega,t) = |\Phi(\omega,r_o)|^2 \frac{8r_o^4 \pi \eta_c}{ct^2} e^{-\omega t/Q} \qquad [20]$$

where $|\Phi(\omega,r_o)|$ represents the amplitude spectra of the backscattering wavelet from a single scatterer located at a reference distance r_o from the source (receiver), η_c is the density of scatterers per unit of volume, c is the wave velocity, and t is lapse time (time after origin time). This equation may be written more simply as

$$P(\omega,t) = S(\omega) \frac{e^{-\omega t/Q_c}}{t^{\mu}} \qquad [21]$$

where the source term $S(\omega)$ contains the effects of both primary and secondary (scattering) sources. It is important to note that $e^{-\omega t/Q}$ in equations (19) and (20) represents attenuation by both intrinsic absorption and scattering and should be written as $e^{-\omega t/Q_c}$.

Additional scattering models such as multiple scattering and diffusion have been developed. While such models may be applied to attenuation studies, a complete discussion of their forms is beyond the scope of this presentation. Excellent summaries of such scattering models and their possible implications for attenuation studies are provided by Sato (1977), Dainty and Toksöz (1981), Pulli (1984), Herraiz and Espinosa (1986), and Rogers and others (1987).

Appendix B. Basic data

The basic data used in this research are digitally recorded short period vertical component seismograms of local and regional seismic events. Triggered signals are demultiplexed, digitized, assigned a filename, and initially stored on a Virginia Tech Seismological Observatory (VTSO) PDP 11/34 processor. Interesting signals are classified as earthquakes, blasts, or other type signals and the event files are archived on magnetic tape. Digital network calibration was completed on 10 April 1986, so only data recorded after that date were used in this research. The events used in this study are listed by VTSO computer filename in Table 8.

Table 8. Seismogram computer files used in this study.

FILENAME	FILE HEADING
860851635.VTF	LOCAL EQKE
873250103.VTF	CARROLL CO., VA EARTHQUAKE
873311859.VTF	WISE COUNTY, VA, THANKSGIVING
880471527.VTF	WASHINGTON COUNTY, VA EARTHQUAKE
861092033.VTF	REGIONAL BLAST
861171242.VTF	REGIONAL SIGNAL
861502047.VTF	REGIONAL BLAST
861642054.VTF	REGIONAL EVENT (EQKE?)
861642119.VTF	REGIONAL BLAST (EQKE?)
861662134.VTF	LARGE REGIONAL EVENT
861821502.VTF	REGIONAL BLAST
862101946.VTF	REGIONAL BLAST
862132312.VTF	REGIONAL BLAST
862322325.VTF	REGIONAL BLAST
870860730.VTF	EASTERN TENNESSEE:29:47.70
871920005.VTF	SE TN (KNOXVILLE?)
880090109.VTF	EQ SW OF NET
880490038.VTF	EQ - CHEROKEE CO. NC
862351740.VTF	LOCAL BLAST
870361638.VTF	HI-TEST BIG BLAST (?)

Appendix C. Windowing Techniques

For the spectral analysis performed in this study, windows of digitally recorded seismic signals were transformed into the frequency domain by the use of Fourier transforms. Different tapering techniques were applied to the time windows to determine which, if any, window is best suited for this analysis. Three events were studied - 862101946, 862132312, and 880471527.

Five different tapers were applied to the Lg windows before the Fourier transforms were calculated: a boxcar, a five percent cosine taper on both ends of the window, a Hamming taper, a Hanning taper, and a boxcar with the start time tapered ten percent. Two tests were performed to evaluate the effect of the tapering. The Lg amplitude spectra produced by the Fourier transforms were plotted for a given station and the shapes of the spectra were compared, Figure 25. The Hanning and Hamming tapers produced slightly smoother spectra than the others. Such smoothness was considered desirable for the study of amplitude decay.

The second test of the windowing techniques was a comparison of Q_{L_g} estimates obtained when tapering the data different ways. A comparison of Q_{L_g} versus frequency plots indicates that the Q_{L_g} results do not vary significantly, Figure 26.

The windows tested were 20 second Lg windows starting with the arrival of a 3.5 km/sec wave. This earliest part of the Lg phase may be contaminated by the S wave coda of the signals studied. The Hanning and Hamming tapers weight this early part of the window less than later parts, less-

ening the possible effect of S wave contamination. These tapers also weight the latter part of the window less, which may help in lessening the effect of the increased scattering component in the latter part of the Lg phase.

Based on the two windowing tests, it was determined that the type of taper applied to the signal windows does not have a significant effect on the final results of the attenuation study. The relatively smooth spectra generated by the Hamming and Hanning tapers are preferred. These two tapers also lessen the effect of possible S wave contamination in the early part of the Lg phase and possible scattering contamination in the latter part of the Lg phase. Because other researchers of coda waves and Lg amplitude decay have used Hanning windows (Hasegawa, 1985; Phillips and Aki, 1986) that type of taper was used in this study.

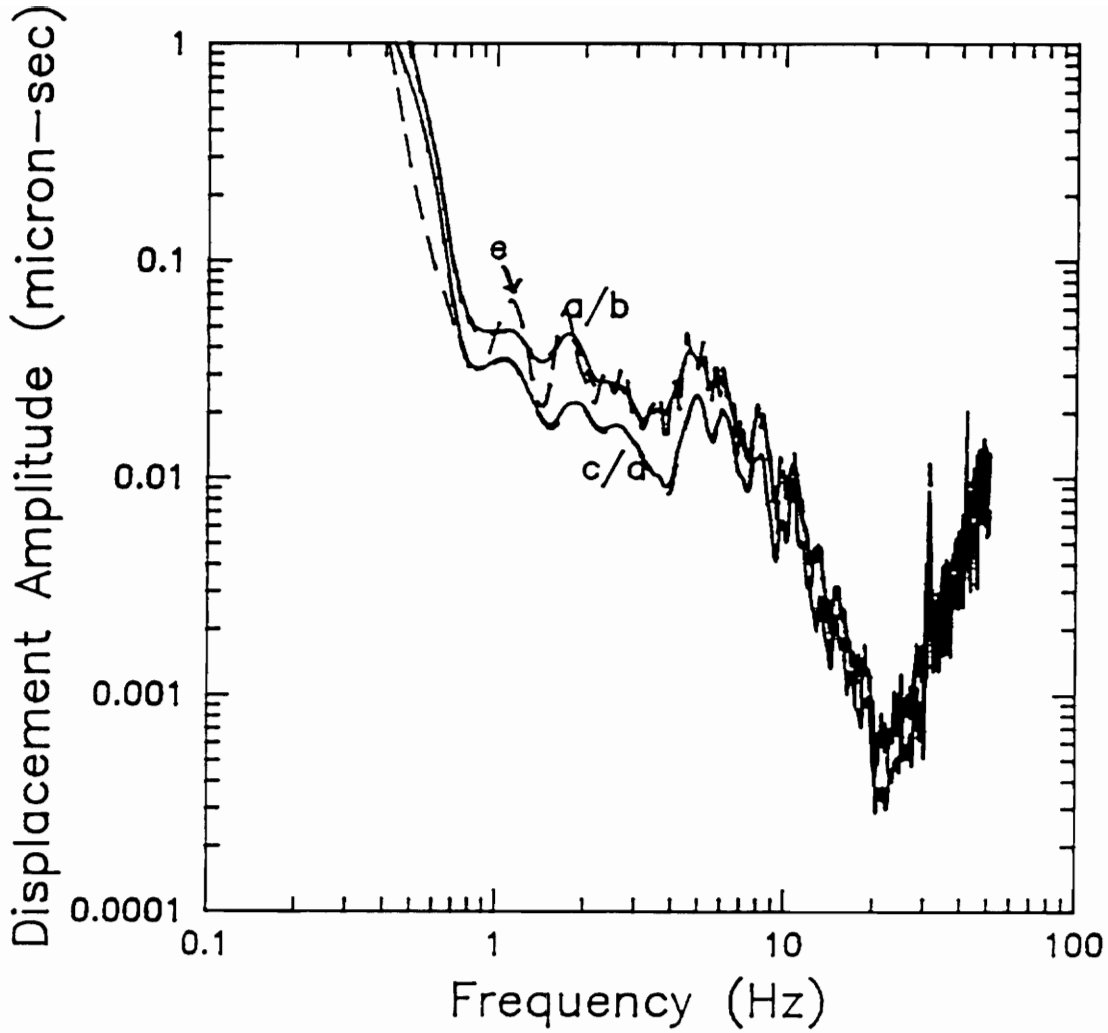

Figure 25. Amplitude spectra generated using the different windows tested: Spectra generated using the five tapers tested: a) Boxcar, b) Five percent cosine, c) Hamming, d) Hanning, e) ten percent initial tapered boxcar.

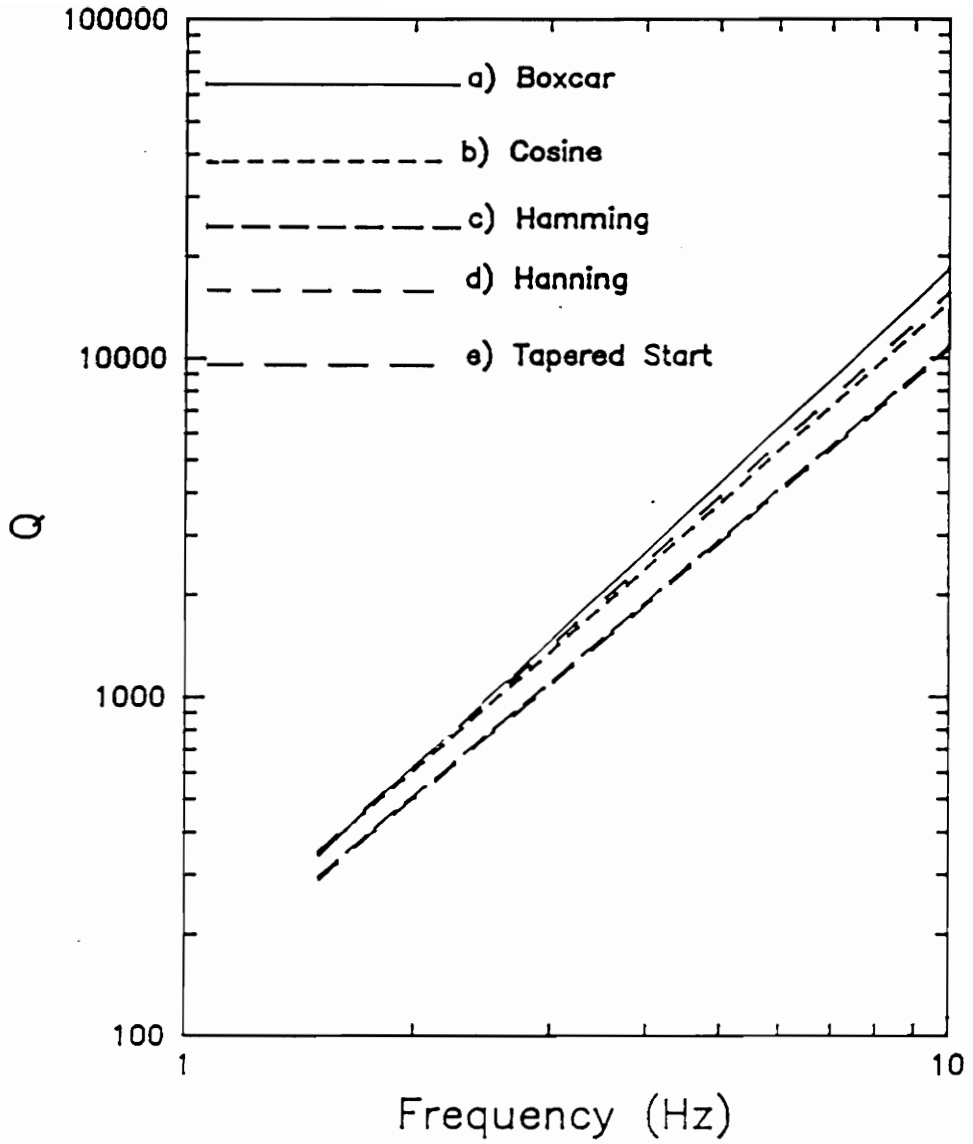

Figure 26. Q_{L_e} values generated using the different windows tested: Q_{L_e} plots generated using the five tapers tested: a) Boxcar, b) Five percent cosine, c) Hamming, d) Hanning, e) ten percent initial tapered boxcar.

Appendix D. Relative Station Site Responses

Relative station site responses, calculated as discussed in the *Site Effects* section of the body of the text, are presented here for stations of the Virginia Tech Seismological Observatory. Only those stations recording ten or more of the Lg data base events were used in the residual analysis.

Station	Common Logarithms of Relative Site Response at Given Frequency (Hz)				
	1.5	**3.0**	**6.0**	**9.0**	**12.0**
HWV	-.0283	.0015	.0299	.-487	.1531
PWV	-.0717	.0039	-.0126	.0167	.042
WMV	-.0231	.0808	.064	.1033	.0627
PUVZ	-.0869	-.098	.0159	.0481	.0921
BLAZ	.1824	-.0035	-.1865	-.2893	-.3263
VWV	.2876	.0973	.0891	-.0189	-.1903
GHV	.0138	.0505	.2833	.2633	.2294
NA2	-.051	-.0738	-.0616	-.0885	-.0906
NA5	.0667	-.0052	-.0045	.0719	.0517
NA12	-.0604	-.0681	-.243	-.33	-.2123

While these station site responses are considered to be relative to the mean values for any one event, we believe that they are fairly accurate representations of the VTSO station site effects. The greatest effect on amplitude that these responses should have is a factor of three. This large an effect would only be seen in limited situations, such as station HWV in the higher frequency range (9-12 Hz). The apparent amplification of low ($\simeq$1 Hz) frequencies at station VWV, predicted by the calculated station site responses, can be observed visually on VTSO seismograms. VWV is located on a topographic promontory and that positioning may cause selective amplification of seismic waves. Data from VWV were often deleted from Q_{L_g} analysis because of large spectral values at 1 Hz on the amplitude spectra plots.

References

Aki, K. (1969). Analysis of seismic coda of local earthquakes as scattered waves. *J. Geophys. Res.*, Vol. 74, pp. 615-631.

Aki, K. and P. G. Richards (1980). *Quantitative seismology - Theory and methods, Volume I*, Freeman and Co., San Francisco, CA, 557 pp.

Ben-Menahem, A. and S. J. Singh (1981). *Seismic waves and sources*, Springer-Verlag, 1108 pp.

Bullen, K. E. and B. A. Bolt (1985). *An introduction to the theory of seismicity*, Cambridge University Press, 499 pp.

Dainty, A. M. and M. N. Toksöz (1981). Seismic codas on the Earth and the Moon: A comparison. *Phys. Earth Planet. Interiors*, Vol. 26, pp. 250-260.

Ewing, W. M., W. S. Jardetzky, and F. Press (1957). *Elastic waves in layered media.* McGraw Hill, New York, 380 pp.

Hasegawa, H. S. (1985). Attenuation of Lg waves in the Canadian Shield. *Bull. Seis. Soc. Amer.*, Vol. 75, No. 6, pp. 1569-1582.

Herraiz, M. and A. F. Espinosa (1986). Scattering and attenuation of high-frequency seismic waves: Development of the theory of coda waves. *USGS Open-File Report 86-455*, 92 p.

Phillips, W. S. and K. Aki (1986). Site amplification of coda waves from local earthquakes in central California. *Bull. Seis. Soc. Amer.*, Vol. 76, pp. 627-648.

Pulli, J. J. (1984). Attenuation of coda waves in New England. *Bull. Seis. Soc. Amer.*, Vol. 74, No. 4, pp. 1149-1166.

Rogers, A. M., S. C. Harmsen, R. B. Herrmann, and M. E. Meremonte (1987). A study of ground motion attenuation in the southern Great Basin, Nevada - California, using several techniques for estimates of Q_s, $\log A_o$, and coda Q. *J. Geophys. Res.*, Vol. 92, No. B5, pp 3527-3540.

Sato, H. (1977). Energy propagation including scattering effects- single isotropic scattering approximation. *J. Phys. Earth,* Vol. 25, pp. 27-41.

Stacey, F. D., M. T. Gladwin, B. McKavanagh, A. T. Linde, and L. M. Hastie (1975). Anelastic damping of acoustic and seismic pulses. *Geophysical Surveys*, Vol. 2, pp. 133-151.

Vita

Melissa Jane Bodé was born on 8 April 1963 in Bristol, Pennsylvania. From September 1963 on she lived in Yardley, PA. She graduated in June 1981 from Pennsbury High School in Fairless Hills, PA and entered Virginia Polytechnic Institute and State University in September, following in her sister's footsteps. She received a B.S. in Geophysics in June 1985 and spent the next four months working at the Hawaiian Volcano Observatory. In January 1986 she returned to Virignia Tech to pursue a Master's Degree in Geophysics. On 5 September 1987 she married Stephen P. Rogers and moved to Huntsville, Alabama.